

Article

# A Novel Improved Cuckoo Search Algorithm for Parameter Estimation of Photovoltaic (PV) Models

Tong Kang <sup>1,\*</sup> , Jiangan Yao <sup>1</sup>, Min Jin <sup>2</sup>, Shengjie Yang <sup>3</sup> and ThanhLong Duong <sup>4</sup>

<sup>1</sup> College of Electrical and Information Engineering, Hunan University, Changsha 410082, China; yaojiangan@126.com

<sup>2</sup> College of Computer Science and Electronic Engineering, Hunan University, Changsha 410082, China; jinmin@hnu.edu.cn

<sup>3</sup> College of Computer and Information Engineering, Hunan University of Commerce, Changsha 410205, China; yangsj16@hotmail.com

<sup>4</sup> Department of Electrical Engineering, Industrial University of Ho Chi Minh City, Ho Chi Minh City 700000, Vietnam; thanhlong802003@yahoo.com

\* Correspondence: kangtong126@126.com; Tel.: +86-731-8882-4089

Received: 30 March 2018; Accepted: 23 April 2018; Published: 25 April 2018



**Abstract:** Parameter estimation of photovoltaic (PV) models from experimental current versus voltage (I-V) characteristic curves acts a pivotal part in the modeling a PV system and optimizing its performance. Although many methods have been proposed for solving this PV model parameter estimation problem, it is still challenging to determine highly accurate and reliable solutions. In this paper, this problem is firstly transformed into an optimization problem, and an objective function (OF) is formulated to quantify the overall difference between the experimental and simulated current data. And then, to enhance the performance of original cuckoo search algorithm (CSA), a novel improved cuckoo search algorithm (ImCSA) is proposed, by combining three strategies with CSA. In ImCSA, a quasi-opposition based learning (QOBL) scheme is employed in the population initialization step of CSA. Moreover, a dynamic adaptation strategy is developed and introduced for the step size without Lévy flight step in original CSA. A dynamic adjustment mechanism for the fraction probability ( $P_a$ ) is proposed to achieve better tradeoff between the exploration and exploitation to increase searching ability. Afterwards, the proposed ImCSA is used for solving the problem of estimating parameters of PV models based on experimental I-V data. Finally, the proposed ImCSA has been demonstrated on the parameter identification of various PV models, i.e., single diode model (SDM), double diode model (DDM) and PV module model (PMM). Experimental results indicate that the proposed ImCSA outperforms the original CSA and its superior performance in comparison with other state-of-the-art algorithms, and they also show that our proposed ImCSA is capable of finding the best values of parameters for the PV models in such effective way for giving the best possible approximation to the experimental I-V data of real PV cells and modules. Therefore, the proposed ImCSA can be considered as a promising alternative to accurately and reliably estimate parameters of PV models.

**Keywords:** photovoltaic modeling; parameter estimation; optimization problem; metaheuristic; opposition-based learning; quasi-opposition based learning; improved cuckoo search algorithm

## 1. Introduction

In recent years, several reasons such as gradually depleting fossil fuel resources, environmental protection concerns, and political issues have resulted in a high demand for electrical energy [1]. Thus, the conflict between the vigorously increasing power demands and scarcity of fossil resource is becoming more and more serious, promoting the development of renewable energy resources,

especially solar energy [2,3]. Since solar energy is emission-free, freely available, and easy to install, the use of solar energy via photovoltaic (PV) systems has attracted great attention all over the world [4,5]. Lately reported by the Photovoltaic Power Systems Programme of the International Energy Agency (IEA PVPS) [6], the global solar PV capacity at the end of 2016 amounted to about 300 GW, with a 50% growth bringing the additional installed solar PV capacity worldwide to at least 75 GW. Three countries, namely China, USA and Japan represented the largest solar PV markets in 2015 as well as 2016, in which there was a 75% increase in newly installed solar PV capacity. Meanwhile, the Asia Pacific region installed more than 66% of the global solar PV capacity in 2016, where China (with at least 34 GW installed) ranked first. Many countries were increasing their installed PV capacity during 2016, which is still going on. With dozens of countries developing solar PV now, and much more to come, the globalization of PV is now a reality. So far, no other single energy technology has shown such a distributed set-up and modularity as PV systems [7]. However, in PV systems, solar PV cells or modules are applied for harnessing the Sun's energy and turn it into electricity. In particular the solar PV cell/module is the most important part of a PV system [8]. Therefore, with regard to the modeling a PV system and optimizing its performance, an accurate modeling of PV cells or modules is necessary.

The modeling of PV cells or modules consists of three major processes: choice of proper electrical circuit models, the expression of mathematical models and precise estimation of values of parameters for them. Although various equivalent electronic circuit models were proposed years ago, in practice, the SDM and the DDM are two most commonly adopted models [9–11]. For the mathematical model, the I-V characteristic that describes PV cell/module behavior is taken into account, and the current equation of PV model is an implicit transcendental equation [10]. Therefore, under the circumstances, a precise parameter estimation of such models is extremely essential and hard work and has drawn much attention recently [11].

Various approaches have been proposed for solving the PV models parameter identification problem, mainly classified into three categories: analytical methods, numerical methods and metaheuristic methods. In analytical methods, the Lambert W-function-based method was applied for estimating solar cells' parameters in [12]. In [13], a novel technique based on Taylor's series expansion was presented to obtain the explicit single-diode model of solar cells. Although analytical methods are simple and can provide rapid solution, they are not flexible and especially, making approximations in them often reduces accuracy. In numerical methods, the Newton-based method was proposed to obtain the parameters of solar cell [14]. In [15,16], the Gauss–Seidel-based method was used to identify the parameters for a SDM of a PV module. The Levenberg-Marquardt (LM) algorithm was employed for estimating five parameters of the SDM of PV modules in [17]. Although numerical methods can offer accurate results, their accuracy relies on the selection of the initial values. Moreover, they may easily trap into local optima. In [18], a new strategy based on the reduced forms of the five-parameter model was proposed for solving the problem of identification of the five unknown parameters from the experimental I-V data of the PV panel. Using the reduced forms, the dimension of the search space can be reduced from five unknown parameters to two. Moreover, the original nonconvex optimization problem can be transformed into a convex optimization problem and any kind of deterministic approach can easily and efficiently find the solution. The capabilities of the proposed reduced forms were verified on two case studies. Comparison results showed the high performances of the novel techniques based on reduced forms. The metaheuristic methods have been widely used for the PV models parameter estimation problem [19–34]. Such methods include genetic algorithm (GA) [19], chaos particle swarm optimization (CPSO) [20], pattern search (PS) [21,22], simulated annealing (SA) [23], harmony search (HS) [1], artificial bee swarm optimization (ABSO) [24],  $R_{cr}$ -IJADE [25], mutative-scale parallel chaos optimization algorithm (MPCOA) [26], biogeography-based optimization algorithm with mutation strategies (BBO-M) [27], artificial bee colony (ABC) [2], modified artificial bee colony (MABC) [28], improved artificial bee colony (IABC) [29], chaotic asexual reproduction optimization (CARO) [4], EHA-NMS [30], generalized oppositional teaching learning based

optimization (GOTLBO) [10], self-adaptive teaching-learning-based optimization (SATLBO) [31], improved JAYA (IJAYA) [32], modified simplified swarm optimization (MSSO) [33], chaotic improved artificial bee colony (CIABC) [11], and teaching-learning-based artificial bee colony (TLABC) [34]. These metaheuristic methods are very flexible and can achieve satisfied results, however, in the light of “no free lunch” (NFL) theorem, there is no single metaheuristic method best suited for all optimization problems [35]. That is to say, a particular algorithm provides best results for a set of problem, while the same algorithm may give the worst performance on a different set of problems. Therefore, searching for the new and most accurate and reliable metaheuristic method for solving PV models parameter estimation problem is still ongoing and always appreciated.

Recently, a new metaheuristic algorithm called cuckoo search algorithm (CSA) is developed by Yang and Deb [36] inspired from the obligate brood parasitic behavior of some cuckoo species and some birds’ Lévy flight characteristic. It has a simple structure, a few control parameters and is easy for users to implement [37]. The CSA uses a control parameter called fraction probability or discovery rate,  $P_a$  to balance the global exploration and local exploitation [38]. Thus, the CSA has attracted great attention of researchers and been successfully employed in various problems from different fields [38,39] compared with a variety of optimization algorithms. However, the original CSA suffers from some drawbacks, which have been improved in this study. Firstly, the CSA uses random initialization cuckoo population of host nests, which decreases the global exploration ability, and causes the convergence of original CSA to deteriorate and results in being easy to trap into local optimum, especially when tackling the problem of dimensional increasing. Secondly, the Lévy flight step size in original CSA needs initializing fixed value for both step size scaling factor,  $\alpha$  and distribution factor,  $\beta$  parameters, which cannot be amended in the next iterations. It is important but difficult to tune proper values of such parameters of the Lévy flight step size for the provided problems. In addition, no strategy is used to control over the step size during the process of iteration while obtaining global optimization in original CSA. Thirdly, the original CSA uses fixed value for fraction probability,  $P_a$ . Thus, an ideal value of  $P_a$  needs to be carefully tuned for a given problem, which is not trouble free. The fixed value of such parameter still lacks an appropriate balance between the global search ability and local search capability of original CSA. Hence, it is necessary to overcome these drawbacks and enhance the performance of the original CSA.

Opposition-based learning (OBL) recently introduced by Tizhoosh [40], is a new scheme for machine intelligence and applied for speeding up various optimization algorithms’ convergence and improving the accuracy of their solutions [41], which has attracted a lot of research attention in recent years [42]. The major concept of OBL is the simultaneous consideration of a guess and its corresponding opposite guess which is closer to the global optimum for finding out a better candidate answer to given problems. Nevertheless, recently, researchers introduced the QOBL and established that a quasi-opposite number is more likely to be closer to the solution than an opposite number [43,44]. Thus, the idea of QOBL has also been successfully used to reinforce several global optimization algorithms like DE, GA, PSO, and BBO [42,44].

For addressing the aforementioned drawbacks of original CSA and improving its performance, in this paper, a novel improved cuckoo search algorithm (ImCSA) is proposed, by combining three strategies with original CSA. Firstly, a strategy called QOBL scheme is employed in the population initialization step of CSA to accelerate its convergence and enhance its solution accuracy. Secondly, a dynamic adaptation strategy is developed and introduced for the step size without Lévy flight step in original CSA, which makes the step size with zero parameter initialization adaptively change according to the individual nest’s fitness value over the course of the iteration and the current iteration number. This strategy is useful for optimization with a faster rate. Thirdly, a dynamic adjustment mechanism for the fraction probability or discovery rate ( $P_a$ ) is proposed for providing better tradeoff between the exploration and exploitation to increase searching ability. This paper focuses on the PV models parameter estimation problem. In this paper, this problem is firstly transformed into an optimization problem, and an OF is formulated to quantify the overall difference between the experimental and

simulated current data. And then, a novel improved version of CSA called ImCSA is proposed and employed to solve the problem of estimating the parameters of PV models based on measured I-V data from the real PV cells/modules. Finally, the proposed ImCSA has been demonstrated on the various PV models, i.e., SDM, DDM and PMM. The main contributions of this article are summarized as follows:

- A new improved variant of CSA, known as ImCSA, is proposed for solving the PV models parameter estimation problem based on experimental I-V data.
- A novel improved CSA, named as ImCSA, by combining three strategies with original CSA to enhance its performance is proposed. First, a QOBL scheme is used in the population initialization step of original CSA. Then, a dynamic adaptation strategy is developed and introduced for the step size without Lévy flight step in original CSA. Finally, a dynamic adjustment mechanism for the fraction probability,  $P_a$  is proposed to provide better balance between the global exploration and local exploitation to increase searching ability. The proposed ImCSA is a global optimization method and could be applied to other real-world problems.
- The proposed ImCSA is able to seek out the best parameter values for PV models in such effective way for giving the best possible approximation to the experimental I-V data of real PV cells and modules. Compared with original CSA and other different methods used in recent literature, the superior performance of the ImCSA is confirmed. Therefore, the proposed ImCSA can serve as a potential alternative to accurately and reliably identify PV models parameters.

The remainder of the article is arranged as follows: Section 2 introduces the PV models in this study. The proposed mathematical problem formulation for parameter estimation of PV models is also presented. The original CSA is given in Section 3. The proposed ImCSA and its application for the PV models parameter estimation problem were described in Section 4. Section 5 demonstrates the experimental results and discussion. Section 6 summarizes the conclusions.

## 2. Photovoltaic (PV) Modeling and Problem Formulation

This section firstly describes the modeling of PV cells and modules. Then, the objective function for the problem is detailed.

### 2.1. PV Cell Model

In the literature, various circuit models have been employed for describing the electrical behavior of PV cells, but in practice, only two widely used models, namely, SDM and DDM, are suitable for electrical engineering applications [4,11,24,26]. These two models will be concisely presented in the following subsections.

#### 2.1.1. Single Diode Model

The SDM is the most normally adopted in the researches for describing the static I-V characteristic of a PV cell due to its simplicity and accuracy [32]. The equivalent circuit of SDM is illustrated in Figure 1a. This model comprises a photo generated current source in parallel with a diode, a series resistor to denote the ohmic losses related to load current and a shunt resistor to present the leakage current. Thus, in term of Kirchhoff's current law (KCL), the PV cell terminal current,  $I_t$ , can be expressed by:

$$I_t = I_{ph} - I_d - I_{sh} \quad (1)$$

where  $I_{ph}$  denotes the photo generated current,  $I_d$  denotes the diode current, and  $I_{sh}$  denotes the shunt resistor current, respectively. Additionally, in term of Shockley equation,  $I_d$  is computed by:

$$I_d = I_{sd}[\exp(q(V_t + I_t R_s)/akT) - 1] \quad (2)$$

where  $I_{sd}$  is the reverse saturation current of diode,  $V_t$  is the cell terminal voltage,  $R_s$  is the series resistance,  $a$  is the diode ideality factor,  $k$  is the Boltzmann constant ( $1.380 \times 10^{-23}$  J/K),  $q$  is the electronic charge ( $1.602 \times 10^{-19}$  C), and  $T$  is the PV cell absolute temperature in Kelvin, respectively. Moreover, using Kirchhoff's voltage law (KVL),  $I_{sh}$  is obtained as:

$$I_{sh} = (V_t + I_t R_s) / R_{sh} \quad (3)$$

where  $R_{sh}$  is the shunt resistance. Therefore, by substituting from Equations (2) and (3) into Equation (1), the I-V relationship of the SDM can be rewritten as follows [2,11]:

$$I_t = I_{ph} - I_{sd} [\exp(q(V_t + I_t R_s) / akT) - 1] - (V_t + I_t R_s) / R_{sh} \quad (4)$$

Consequently, for this SDM, there are five unknown parameters, namely,  $I_{ph}$ ,  $I_{sd}$ ,  $a$ ,  $R_s$ , and  $R_{sh}$  that can be estimated based on experimental I-V data. Accurate estimations of these parameters are vital to reflect the PV cell characteristics closer to the real characteristics, and this can be achieved by an optimization technique.

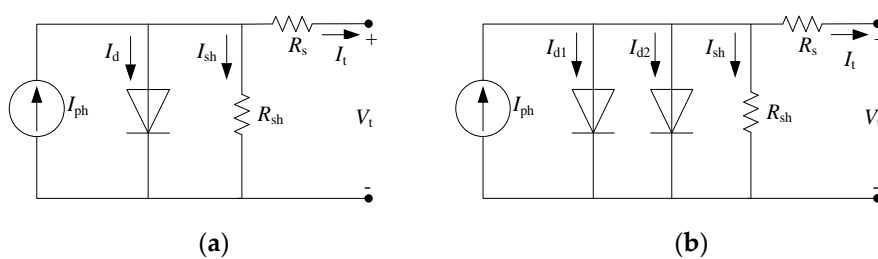


Figure 1. Equivalent circuits of a PV cell: (a) The SDM; (b) The DDM.

### 2.1.2. Double Diode Model

The DDM is the second most widely used circuit model in practice for PV cells. Although the SDM is known to provide a satisfactory approximation to the characteristic of a practical PV cell, the effect of recombination current loss in the depletion region need to be taken into account for making the model more realistic and achieving higher degrees of accuracy. The equivalent circuit of DDM is shown in Figure 1b. This model includes two diodes in parallel with the photo generated current source, a series resistance and a shunt resistance. Hence, by applying KCL,  $I_t$  can be expressed by:

$$I_t = I_{ph} - I_{d1} - I_{d2} - I_{sh} \quad (5)$$

where  $I_{d1}$  denotes the first diode current, and  $I_{d2}$  denotes the second diode current, respectively. In addition, according to the Shockley equation,  $I_{d1}$  and  $I_{d2}$  are given as follows:

$$I_{d1} = I_{sd1} [\exp(q(V_t + I_t R_s) / a_1 kT) - 1] \quad (6)$$

$$I_{d2} = I_{sd2} [\exp(q(V_t + I_t R_s) / a_2 kT) - 1] \quad (7)$$

where  $I_{sd1}$  and  $I_{sd2}$  represent the diffusion and saturation currents, respectively.  $a_1$  and  $a_2$  stand for the diode ideality factors. Thereby, like the SDM, the I-V relationship of the DDM is finally computed by [11,34]:

$$I_t = I_{ph} - I_{sd1} [\exp(q(V_t + I_t R_s) / a_1 kT) - 1] - I_{sd2} [\exp(q(V_t + I_t R_s) / a_2 kT) - 1] - (V_t + I_t R_s) / R_{sh} \quad (8)$$

Obviously, from Equation (8), seven unknown parameters, namely,  $I_{ph}$ ,  $I_{sd1}$ ,  $I_{sd2}$ ,  $a_1$ ,  $a_2$ ,  $R_s$ , and  $R_{sh}$  need to be identified based on the given I-V data from a real PV cell. Therefore, this is a crucial task

in PV systems to accurately estimate such values of parameters for ensure a better performance of a practical PV cell.

## 2.2. PV Module Model

The PMM that comprises of several PV cells interconnected in series and/or in parallel to raise the level of output voltage and/or current [4,21–23,26]. The equivalent circuit model of a PV module (based on SDM) is depicted in Figure 2. Therefore, the Equation (4) of SDM is directly employed to express the I-V relationship of a PMM as follows:

$$I_t = I_{ph}N_p - I_{sd}N_p [\exp(q(V_t + I_tR_sN_s/N_p)/aN_s kT) - 1] - (V_t + I_tR_sN_s/N_p)/R_{sh}N_s/N_p \quad (9)$$

where  $N_s$  and  $N_p$  denote the number of PV cells in series and parallel, respectively.

Considering the concision, Equation (9) is also rewritten as:

$$I_t = I_{phm} - I_{sdm} [\exp(q(V_t + I_tR_{sm})/a_m kT) - 1] - (V_t + I_tR_{sm})/R_{sh_m} \quad (10)$$

where  $I_{phm} = I_{ph}N_p$ ,  $I_{sdm} = I_{sd}N_p$ ,  $a_m = aN_s$ ,  $R_{sm} = R_sN_s/N_p$ , and  $R_{sh_m} = R_{sh}N_s/N_p$ , respectively.

Considering this PV module model based on SDM, five unknown parameters, namely,  $I_{phm}$ ,  $I_{sdm}$ ,  $a_m$ ,  $R_{sm}$ , and  $R_{sh_m}$  must be estimated based on the given I-V data of real PV modules. Similarly, an accurate identification of these parameters is critical to optimizing the performance of a PV module.

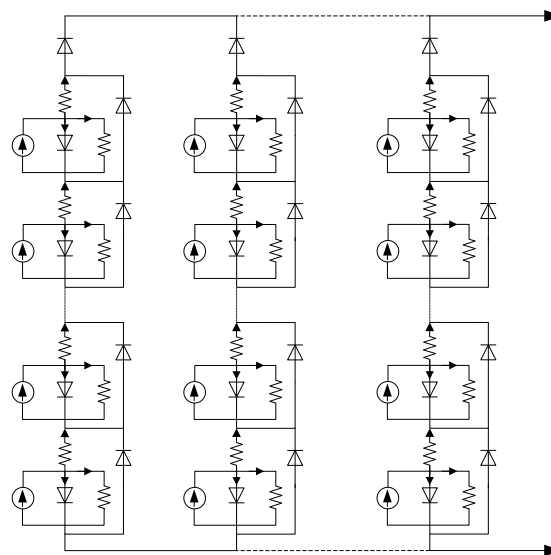


Figure 2. Equivalent circuit model of a PV module.

## 2.3. Objective Function

The main intention of mathematical modeling of PV models is to precisely estimate the values of unknown parameters that characterize several models, especially the aforementioned PV models such as SDM, DDM and PMM, based on measured I-V data from real PV cells and PV modules. However, estimation of the most optimal values of unknown parameters is a difficult and challenge problem since the characteristic current equations describing the PV models are implicit, nonlinear and transcendental [10]. Thus, this PV models parameter estimation problem can be transformed into an optimization problem, in which the aim is to minimize the difference between the experimental I-V data and the I-V data from model computed by taking into consideration a specific set of estimated

parameters. This difference also called error function can be defined by rewriting the Equations (4), (8) and (10) in their homogeneous forms for SDM, DDM and PMM respectively as follows:

$$\begin{cases} e_{SDM}(V_t, I_t, \theta) = I_{ph} - I_{sd}[\exp(q(V_t + I_t R_s)/akT) - 1] - (V_t + I_t R_s)/R_{sh} - I_t \\ \theta = [I_{ph}, I_{sd}, a, R_s, R_{sh}] \end{cases} \quad (11)$$

$$\begin{cases} e_{DDM}(V_t, I_t, \theta) = I_{ph} - I_{sd1}[\exp(q(V_t + I_t R_s)/a_1kT) - 1] - I_{sd2}[\exp(q(V_t + I_t R_s)/a_2kT) - 1] \\ \quad - (V_t + I_t R_s)/R_{sh} - I_t \\ \theta = [I_{ph}, I_{sd1}, I_{sd2}, a_1, a_2, R_s, R_{sh}] \end{cases} \quad (12)$$

$$\begin{cases} e_{PMM}(V_t, I_t, \theta) = I_{phm} - I_{sdm}[\exp(q(V_t + I_t R_{sm})/a_m kT) - 1] - (V_t + I_t R_{sm})/R_{shm} - I_t \\ \theta = [I_{phm}, I_{sdm}, a_m, R_{sm}, R_{shm}] \end{cases} \quad (13)$$

where  $e(V_t, I_t, \theta)$  is the error function which means the difference between the simulated current using model determined by estimated parameters and experimental current from a PV cell and module, and computed for each pair of the measured data.  $\theta$  is the solution vector which includes the several unknown parameters of PV models to be identified, where  $\theta = [I_{ph}, I_{sd}, a, R_s, R_{sh}]$  is for the SDM,  $\theta = [I_{ph}, I_{sd1}, I_{sd2}, a_1, a_2, R_s, R_{sh}]$  is for the DDM and  $\theta = [I_{phm}, I_{sdm}, a_m, R_{sm}, R_{shm}]$  is for the PMM, respectively.

Hence, considering that defining an OF is necessary for the optimization problem, we adopt the root mean square error (RMSE) as the OF in our study to quantify the overall difference between the simulated and experimental current data. And this OF has been widely used in the literature [1,2,4,10,11,29], which is formulated as follows:

$$\text{Min OF}(\theta) = \text{Min RMSE}(\theta) = \text{Min} \sqrt{\frac{1}{N} \sum_{i=1}^N (e_i(V_t, I_t, \theta))^2} \quad (14)$$

where  $N$  is the number of measured data points.

Therefore, in our study, the PV models parameter estimation is an optimization process that minimizes the  $\text{OF}(\theta)$  by successively regulating the model parameters solution vector  $\theta$  within the specified search interval. Obviously, the smaller value of the OF, the better the solution is and that is, the more precise the parameter values estimated from the model. Moreover, it is significant that any decrease occurs in the OF value, representing an improvement in the knowledge about the real values of the parameters [24].

### 3. The Original CSA

The CSA is a recent metaheuristic algorithm proposed by Yang and Deb [36]. The main idea behind CSA is the combination of the cuckoo bird's obligate brood parasitic behaviour and some insects' Lévy flights characteristics. To simply give a description of the original CSA, cuckoo search is based on the following three idealized rules [36,38,39]:

- One egg is laid by each cuckoo at a time and dumps its egg into any chosen nest randomly.
- Nests with the best quality eggs are maintained to the forthcoming generations.
- The fraction probability ( $P_a$ ) of the host birds discovering cuckoo's egg lies within probability range  $P_a \in [0, 1]$ . The available host nest is fixed.

Combining cuckoo search based on three idealized rules with Lévy flight phenomenon, the CSA can be easily formed. In CSA, a fraction probability or discovery rate,  $P_a$  is used to balance the global search ability and local search capability. The local search can be expressed by:

$$X_i^{t+1} = X_i^t + \alpha s \otimes H(P_a - \varepsilon) \otimes (X_j^t - X_k^t) \quad (15)$$

where  $X_i, X_j$  and  $X_k$  are three different solutions;  $\alpha > 0$  is the step size scaling factor;  $s$  is the step size;  $\otimes$  means entry-wise multiplications;  $H(\cdot)$  is a Heaviside function and  $\varepsilon$  is a random number uniformly distributed. On the other hand, the global search is conducted by using Lévy flights as:

$$X_i^{t+1} = X_i^t + \alpha L(s, \lambda), \quad L(s, \lambda) = \frac{\lambda \Gamma(\lambda) \sin(\pi\lambda/2)}{\pi} \frac{1}{s^{1+\lambda}}, \quad (s \gg s_0 > 0) \quad (16)$$

where  $\Gamma(\cdot)$  is a Gamma function and expressed by:

$$\Gamma(z) = \int_0^\infty t^{z-1} e^{-t} dt \quad (17)$$

in a special case when  $z = n$  is an integer, then we have  $\Gamma(n) = (n - 1)!$ .

The Lévy flight essentially provides a random walk whose random step length is drawn from a Lévy distribution as:

$$Le'vy \sim \frac{1}{s^{\lambda+1}}, \quad (0 < \lambda \leq 2) \quad (18)$$

which has an infinite variance with an infinite mean.

In Mantegna's algorithm, the step length  $s$  is calculated as [39]:

$$s = \frac{u}{|v|^{\frac{1}{\beta}}} \quad (19)$$

where  $u$  and  $v$  are normally distributed stochastic variables as:

$$\begin{cases} u \sim N(0, \sigma_u^2) \\ v \sim N(0, \sigma_v^2) \end{cases} \quad (20)$$

and  $\sigma_u, \sigma_v$  represent the standard deviations and are given by:

$$\begin{cases} \sigma_u = \left\{ \frac{\Gamma(1+\beta) \sin(\pi\beta/2)}{\Gamma[(1+\beta)/2] \beta 2^{(\beta-1)/2}} \right\}^{1/\beta} \\ \sigma_v = 1 \end{cases} \quad (21)$$

where  $\beta$  is the distribution factor ( $0.3 \leq \beta \leq 1.99$ ).

Hence, the pseudocode of the original CSA is presented in Algorithm 1.

---

**Algorithm 1: Pseudocode of the original CSA**

---

1. Randomly initialize  $n$  host nests within specified range as  $\theta_i$  ( $i = 1, \dots, n$ )
  2. Compute fitness value  $f_i$  ( $i = 1, \dots, n$ )
  3. Determine the global best nest with the best fitness value
  4. for  $It = 1:It_{\max}$
  5.     Randomly generate a new solution (say  $C_i$ ) using Lévy flights
  6.     Compute its fitness value  $f_{tr}$
  7.     Randomly choose a solution (say  $\theta_m$ ) from current  $n$  solutions
  8.     if ( $f_{tr} < f_m$ ) then
  9.          $\theta_m = C_i$
  10.         $f_m = f_{tr}$
  11.     end if
  12.     Drop several worst nests via probability ( $P_a$ ) and build new ones
  13.     Keep the best solutions
  14.     Rank and seek out the current global best nest
  15.    end for
  16. Postprocess results and visualization
-

The major procedure of original CSA can be presented as follows:

1. Randomly initialize  $n$  host nests within specified range:

$$\theta_i = (\theta_{i1}, \theta_{i2}, \dots, \theta_{ij})^T \quad i = 1, 2, \dots, n \quad j = 1, 2, \dots, d \quad (22)$$

where  $\theta_i$  denotes the  $i$ th nest;  $\theta_{ij}$  denotes the  $j$ th element of the  $i$ th nest;  $d$  denotes the dimension. Set the value of discovery rate  $P_a \in [0, 1]$ . Set the maximum number of iterations  $It_{\max}$ .

2. Compute fitness value  $f_i$  ( $i = 1, \dots, n$ ), select the best value of each nest  $\theta_{best_i}$  and the global best nest  $G_{best}$ , memorize fitness values and the best fitness value.
3. Randomly generate a new solution using Lévy flights. As aforementioned, the new solution is given by:

$$\theta_i^{new} = \theta_{best_i} + rand_1 \times S_i^{new} \times (\theta_{best_i} - G_{best}) \quad (23)$$

where  $rand_1$  is a random number drawn from a normal distribution and the step size  $S_i^{new}$  is determined by:

$$S_i^{new} = \alpha \times \frac{u}{|v|^{1/\beta}} \quad (24)$$

where  $\alpha$  is the step size scaling factor and set to 0.01;  $\beta$  is the distribution factor and set to 1.5;  $u$  and  $v$  are two normally distributed stochastic variables ( $u \sim N(0, \sigma_u^2)$  and  $v \sim N(0, \sigma_v^2)$ ) with respective the  $\sigma_u$  and  $\sigma_v$  aforementioned in (21).

4. Compute the fitness values of the new solutions, decide the newly  $\theta_{best_i}$  and  $G_{best}$  via comparing the memorized fitness values in Step 2 with newly computed ones, update  $\theta_{best_i}$  and  $G_{best}$ , and memorize fitness values and the best fitness value.
5. Drop several worst nests via probability ( $P_a$ ) and build new solution. Due to this action, the new solution can be calculated by:

$$\theta_i^{disc} = \theta_{best_i} + C \times \Delta\theta_i^{disc} \quad (25)$$

where  $C$  is the updated coefficient resolved by  $P_a$  and given by:

$$C = \begin{cases} 1 & \text{if } rand_2 < P_a \\ 0 & \text{otherwise} \end{cases} \quad (26)$$

and the increased value  $\Delta\theta_i^{disc}$  is computed by:

$$\Delta\theta_i^{disc} = rand_3 \times [rand_{p_1}(\theta_{best_i}) - rand_{p_2}(\theta_{best_i})] \quad (27)$$

where  $rand_2$  and  $rand_3$  are random numbers drawn from normal distributions;  $rand_{p_1}(\theta_{best_i})$  and  $rand_{p_2}(\theta_{best_i})$  are the random perturbation for positions of nests in  $\theta_{best_i}$ .

6. Compute the fitness values of the new solutions, decide the newly  $\theta_{best_i}$  and  $G_{best}$  via comparing the computed fitness values of these new solutions with memorized fitness values in Step 4, update  $\theta_{best_i}$  and  $G_{best}$ , memorize fitness values and the best fitness value.
7. If the predefined maximum number of iterations  $It_{\max}$  is reached, stop the calculation and display the results, else go to Step 3.

#### 4. The Proposed Novel Improved Cuckoo Search Algorithm (ImCSA) and Its Application

In this section, the novel improved cuckoo search algorithm (ImCSA) is firstly proposed, by combining three strategies with CSA to enhance the performance of the original CSA. Then, we present the procedure of employing the proposed ImCSA to solve the problem of PV models parameter estimation.

#### 4.1. Proposed ImCSA

The ImCSA is proposed in this subsection. Three main strategies as improvements of the original CSA exist in the ImCSA. First, a QOBL scheme is employed in the population initialization step of CSA to accelerate its convergence and enhance its solution accuracy. Second, a dynamic adaptation strategy is developed and introduced for the step size without Lévy flight step in original CSA, which makes the step size with zero parameter initialization adaptively change according to the individual nest's fitness value over the course of the iteration and the current iteration number. This strategy is useful for optimization with a faster rate. Third, a dynamic adjustment mechanism for the fraction probability or discovery rate ( $P_a$ ) is proposed to provide better tradeoff between the exploration and exploitation to increase searching ability. These three main strategies in the ImCSA are elucidated in the following subsections and the implementation of the proposed ImCSA is finally described.

##### 4.1.1. Quasi-Opposition Based Learning Scheme for the Population Initialization

As mentioned in Section 3, the original CSA adopts random initialization cuckoo population of host nests. This random initialization population method decreases the global exploration ability, which causes the convergence of original CSA to deteriorate and results in being easy to fall into local optimal solution. Here, to overcome this drawback, a strategy called QOBL scheme is introduced to accelerate convergence rate and enhance the solutions quality of CSA.

The OBL recently introduced by Tizhoosh [40], is a new scheme for machine intelligence and applied for speeding up various optimization algorithms' convergence and improving the accuracy of their solutions [41]. The major concept of OBL is the simultaneous consideration of a guess and its corresponding opposite guess which is closer to the global optimum for finding out a better candidate answer to given problems.

In general, all population-based optimization algorithms start with some initial solutions and try to improve them toward some optimal solution(s). The process of searching stops when several predefined criteria are satisfied. We usually start with random estimations for the absence of a priori knowledge or information about the solution. Researchers have established that an opposite candidate solution has a higher probability of being closer to the global optimum than a random candidate solution [41]. Hence, starting with the closer of the two guesses has the potential to speed up convergence and improve solution's accuracy. Recently, researchers introduced QOBL [43,44] and established that a quasi-opposite number is more likely to be closer to the solution than an opposite number.

In order to easily explain OBL and QOBL, we need to define some concepts clearly. The opposite number and opposite point adopted for OBL are defined by [41]:

1. Opposite number: Let  $X \in R$  be a real number defined on a certain interval:  $X \in [a, b]$ .

The opposite number  $\overset{\circ}{X}$  is defined by:

$$\overset{\circ}{X} = a + b - X \quad (28)$$

2. Opposite point: Let  $P = (X_1, X_2, \dots, X_n)$  be a point in n-dimensional space, where  $X_1, X_2, \dots, X_n \in R$  and  $X_i \in [a_i, b_i] \forall i \in \{1, 2, \dots, n\}$ . The opposite point  $\overset{\circ}{P} = (\overset{\circ}{X}_1, \overset{\circ}{X}_2, \dots, \overset{\circ}{X}_n)$  is completely defined by its components  $\overset{\circ}{X}_1, \overset{\circ}{X}_2, \dots, \overset{\circ}{X}_n$  where:

$$\overset{\circ}{X}_i = a_i + b_i - X_i \quad (29)$$

Here, the quasi-opposite number and quasi-opposite point adopted for QOBL are defined by [43]:

1. Quasi-opposite number: Let  $X \in R$  be a real number defined on a certain interval:  $X \in [a, b]$ . The quasi-opposite number  $\widetilde{X}^{qo}$  is defined by:

$$\widetilde{X}^{qo} = rand((a + b)/2, \widetilde{X}^o) \quad (30)$$

where  $\widetilde{X}^o$  is the opposite number of  $X$ ;  $rand((a + b)/2, \widetilde{X}^o)$  is a random number uniformly distributed between  $(a + b)/2$  and  $\widetilde{X}^o$ .

2. Quasi-opposite point: Let  $P = (X_1, X_2, \dots, X_n)$  be a point in  $n$ -dimensional space, where  $X_1, X_2, \dots, X_n \in R$  and  $X_i \in [a_i, b_i] \forall i \in \{1, 2, \dots, n\}$ . The quasi-opposite point  $\widetilde{P}^{qo} = (\widetilde{X}_1^{qo}, \widetilde{X}_2^{qo}, \dots, \widetilde{X}_n^{qo})$  is completely defined by its components  $\widetilde{X}_1^{qo}, \widetilde{X}_2^{qo}, \dots, \widetilde{X}_n^{qo}$  where:

$$\widetilde{X}_i^{qo} = rand((a + b)/2, \widetilde{X}_i^o) \quad (31)$$

where  $\widetilde{X}_i^o$  is the opposite point of  $X_i$ ;  $rand((a_i + b_i)/2, \widetilde{X}_i^o)$  is a random point uniformly distributed between  $(a + b)/2$  and  $\widetilde{X}_i^o$ .

Overall, in our paper, for improving the performance of original CSA, the QOBL scheme is chosen and employed in the population initialization step of the original CSA. By considering a guess and its corresponding quasi-opposite guess simultaneously, the QOBL scheme leads to searching of search space more thoroughly, which can provide a faster rate of convergence and a higher probability of seeking candidate solutions closer to the global optimum.

#### 4.1.2. Dynamic Adaptation Strategy for the Step Size

Accordingly, in CSA, the global exploration phase for generation of new eggs is governed by Lévy flight based random walks and one has to define the Lévy flight step size. However, in the literature [38,39], the Lévy flight step size needs initializing fixed value for both step size scaling factor,  $\alpha$  and distribution factor,  $\beta$  parameters, which cannot be amended in the next iterations. Moreover, the characteristics of the next generation nests are decided by step size scaling factor,  $\alpha$  and fraction probability,  $P_a$  in original CSA. On one hand, if the fixed value of  $\alpha$  is set too large, the iterations of algorithm will considerably increase while the rate of convergence cannot be guaranteed. Consequently, the host nest will fly beyond boundaries, out of search space, which will affect the accuracy of solution. On the other hand, though a small value of  $\alpha$  leads to a high speed convergence rate, it may be unable to seek out global optimum.

Hence, it is crucial and difficult to choose an appropriate value of the step size scaling factor  $\alpha$  of the Lévy flight step size for a given problem. Additionally, there is no strategy to control over the step size during the process of iteration while obtaining global optimization by using an original CSA. In order to overcome these drawbacks, we ignore the parameters. Here, a dynamic adaptation strategy is developed and introduced for the step size without Lévy flight step in original CSA. In this sense, the step size  $S_i^{new}$  can be modeled as follows:

$$S_i^{new} = \left( \frac{1}{It} \right)^{\left| \frac{Bestf(It) - f_i(It)}{Bestf(It) - Worstf(It)} \right|} \quad (32)$$

where  $It$  is the current iteration number;  $Bestf(It)$  is the best fitness value in the iteration  $It$ ;  $f_i(It)$  is the fitness value of  $i$ th nest in the iteration  $It$ ;  $Worstf(It)$  is the worst fitness value in the iteration  $It$ .

Quite evidently, as can be seen from Equation (32), the step size is now with zero parameter to be initialized, which not only relies on the current iteration number but also relies on the fitness value of individual nest in the search space. It is obvious that the step size is automatically determined during the iterative search process of the algorithm and adaptively changed according to the individual nest's

fitness value over the course of the iteration and the current iteration number. Therefore, though the step size is large at the beginning, when the number of the iteration increases, the step size decreases. That is to say, the step size is very small, when the algorithm reaches to the global optimum. Thus, in our study, the dynamic adaptation strategy for the step size without Lévy flight step in original CSA has been investigated and is beneficial to optimization with a faster rate and higher quality solutions.

#### 4.1.3. Dynamic Adjustment Mechanism for the Fraction Probability

As a matter of fact, considering the search process, the original CSA uses a combination of global explorative Lévy flight based random walk and local exploitative random walk which is controlled by fraction probability or discovery rate,  $P_a$ . From the viewpoint of fraction probability  $P_a$ , the large value of  $P_a$  leads to increase the diversity of solutions and inhibit premature convergence, while the small value of  $P_a$  will increase search accuracy but slow down the search process.

However, the original CSA uses fixed value for fraction probability,  $P_a$ . Thus, an ideal value of  $P_a$  needs to be carefully tuned for a given problem, which is not trouble free. The fixed value of  $P_a$  still lacks an appropriate balance between the global search ability and local search capability of original CSA. To overcome this problem and improve the search ability, in this paper, a dynamic adjustment mechanism is introduced into the original CSA to realize the dynamic control of the fraction probability or discovery rate,  $P_a$ , which is calculated as follows:

$$P_a = P_{a,\max} - (P_{a,\max} - P_{a,\min}) \times \frac{It}{It_{\max}} \quad (33)$$

where  $P_{a,\max}$  is the maximum fraction probability and equal to 0.25;  $P_{a,\min}$  is the minimum fraction probability and equal to 0.01;  $It$  and  $It_{\max}$  are the current iteration number and the maximum number of iterations, respectively.

#### 4.1.4. Implementation of the Proposed ImCSA

In this paper, for further enhancing the performance of CSA, a novel ImCSA is proposed based on three strategies detailed above. First, a QOBL scheme is used in the population initialization step of original CSA. Then, a dynamic adaptation strategy is developed and introduced for the step size without Lévy flight step in original CSA. Finally, a dynamic adjustment mechanism for the fraction probability,  $P_a$  is proposed to achieve better tradeoff between the global exploration and local exploitation to increase searching ability. In addition, the proposed ImCSA has a simple structure and is thus easy for user to implement, which is the same as that of original CSA. The implementation processes of the proposed ImCSA can be presented as the pseudocode listed in Algorithm 2. Newly added/extended code segments are highlighted in bold.

---

#### Algorithm 2: Pseudocode of the proposed ImCSA

---

**/\* QOBL scheme for the population initialization \*/**

1. **Generate uniformly distributed initial  $n$  host nests  $N_0$**
  2. **for  $i = 1:n$  //  $n$ : Host nests size**
  3.   **for  $j = 1:d$  //  $d$ : Problem dimension**
  4.      $ON_{0ij} = a_j + b_j - N_{0ij}$  //  $ON_0$ : **Opposite of initial host nests  $N_0$ ;  $[a_j, b_j]$ : Range of the  $j$ th variable**
  5.      $M_{ij} = (a_j + b_j)/2$  //  $M_{ij}$ : **Middle point**
  6.     **if ( $N_{0ij} < M_{ij}$ )**
  7.        $QON_{0ij} = M_{ij} + (ON_{0ij} - M_{ij}) \times rand(0,1)$  //  $QON_0$ : **Quasi-opposite of initial host nests  $N_0$**
- //rand(0,1): A random number uniformly generated**
-

---

```

8.         else
9.              $QON_{0i,j} = ON_{0i,j} + (M_{i,j} - ON_{0i,j}) \times rand(0,1)$ 
10.        end if
11.    end for
12. end for
13. Choose  $n$  fittest nests from set of  $\{N_0, QON_0\}$  as initial host nests  $N_0$ 
/* End of QOBL scheme for the population initialization */

14. Compute fitness value  $f_i$  ( $i = 1, \dots, n$ )
15. Determine the global best nest with the best fitness value
16. for  $It = 1:It_{max}$ 

/* Dynamic adaptation strategy for the step size */
17. Find the best fitness value  $Bestf(It)$  and the worst fitness value  $Wortf(It)$  in the iteration  $It$ 
18. Randomly generate a new solution (say  $C_i$ ) using Equations (23) and (32)
/* End of dynamic adaptation strategy for the step size */

19. Compute its fitness value  $f_{tr}$ 
20. Randomly choose a solution (say  $\theta_m$ ) from current  $n$  solutions
21. if ( $f_{tr} < f_m$ ) then
22.      $\theta_m = C_i$ 
23.      $f_m = f_{tr}$ 
24. end if

/* Dynamic adjustment mechanism for the fraction probability */
25. Calculate the dynamic adjustment fraction probability ( $P_a$ ) using Equation (33)
/* End of dynamic adjustment mechanism for the fraction probability */

26. Drop several worst nests via probability ( $P_a$ ) and build new ones
27. Keep the best solutions
28. Rank and seek out the current global best nest  $G_{best}$ 
29. end for
30. Postprocess results and visualization

```

---

#### 4.2. Procedure of the Proposed ImCSA-based PV Models Parameter Estimation

This subsection describes the major procedures of employing the proposed ImCSA for solving the PV models parameter estimation problem based on experimental I-V data of real PV cells and modules. The successive steps can be detailed below:

1. Read the  $N$  measured I-V data values of  $V_t$  and  $I_t$  and set associated parameters of the proposed ImCSA such as the host nests size  $n$ , the dynamic adjustment fraction probability  $P_a$  amount within the domain of  $[P_{a,min}, P_{a,max}]$ , the number of variables to be optimized  $d$ , and  $It_{max}$ .
2. Initialize  $n$  host nests  $N_0$  considering the variables to be optimized (the unknown parameters of solar cell models, where the parameters solution vector  $\theta = [I_{ph}, I_{sd}, a, R_s, R_{sh}]$  is for the SDM,  $\theta = [I_{ph}, I_{sd1}, I_{sd2}, a_1, a_2, R_s, R_{sh}]$  is for the DDM, and  $\theta = [I_{phm}, I_{sdm}, a_m, R_{sm}, R_{shm}]$  is for the PMM, respectively). The solution vector  $\theta$  is randomly generated within the specified range which is widely used in the literature [4,25,31,32,34].
3. Create quasi-opposite of initial host nests ( $QON_0$ ) using Equation (31).
4. Evaluate the OF for the initial host nests ( $N_0$ ) and quasi-opposite of initial host nests ( $QON_0$ ) according to the OF( $\theta$ ) in Equation (14).
5. Select  $n$  (host nests size) fittest nests from the initial host nests ( $N_0$ ) and quasi-opposite of initial host nests ( $QON_0$ ) as initial host nests ( $N_0$ ).

6. Evaluate the OF values for  $n$  host nests  $N_0$ , select the best value of each nest  $\theta_{best_i}$  and the global best nest  $G_{best}$  which is corresponding to the best  $OF(\theta)$ , memorize objective values and the best objective value.
7. Find the best objective value  $Bestf(It)$  and the worst objective value  $Worstf(It)$  in the current iteration number  $It$ .
8. Randomly generate a new solution using Equations (23) and (32)
9. Compute the OF values of the new solutions, decide the newly  $\theta_{best_i}$  and  $G_{best}$  via comparing the memorized objective values in Step 6 with newly computed ones, update  $\theta_{best_i}$  and  $G_{best}$ , and memorize objective values and the best objective value.
10. Calculate the dynamic adjustment fraction probability ( $P_a$ ) using Equation (33)
11. Drop several worst nests with a dynamic control of the fraction probability or discovery rate,  $P_a$  and build new solution. Due to this action, the new solution can be calculated using Equations (25)–(27).
12. Compute the OF values of the new solutions, decide the newly  $\theta_{best_i}$  and  $G_{best}$  via comparing the computed  $OF(\theta)$  in Equation (14) of these new solutions with memorized objective values in Step 9, update  $\theta_{best_i}$  and  $G_{best}$ , memorize objective values and the best objective value.
13. If the predefined maximum number of iterations  $It_{max}$  is reached, terminate the computation and display the results (the best solution vector  $\theta$  and the corresponding objective value  $OF$  (RMSE)), else go to Step 7.

The flowchart of the procedure of employing the proposed ImCSA for solving the PV models parameter estimation problem is depicted in Figure 3.

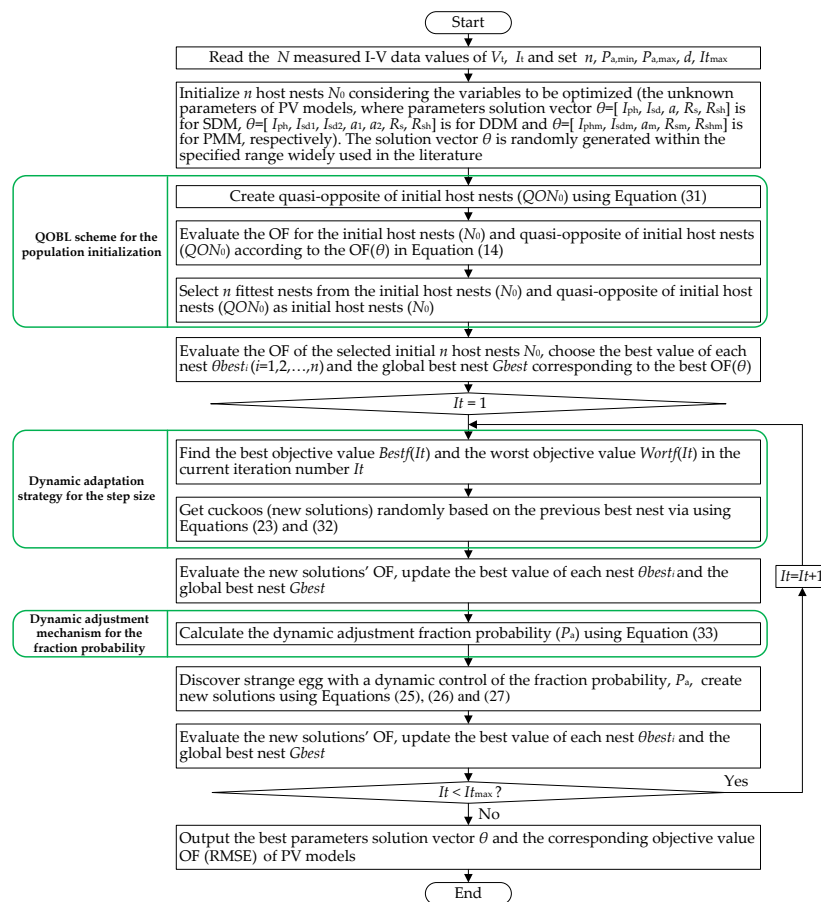


**Figure 3.** The flowchart of the procedure of employing the proposed ImCSA for solving the PV models parameter estimation problem.

## 5. Experimental Results and Discussion

This section is to fully evaluate the performance of proposed ImCSA for parameter estimation of various PV models, i.e., SDM, DDM and PMM. Two datasets of experiments, namely, benchmark datasets of a standard PV cell and a standard PV module, and real datasets of PV panels are used in the following subsections. First, the benchmark datasets of a standard PV cell and a standard PV module are chosen to verify the effectiveness of proposed ImCSA and compare with the results reported in literature. The benchmark datasets are acquired from [14], where the experimental I-V data are measured using a 57 mm diameter commercial RTC (the R.T.C. Company, Paris, France) France silicon solar cell (under a  $1000 \text{ W/m}^2$  irradiance and  $33 \text{ }^\circ\text{C}$  temperature) and a PV module named Photowatt-PWP201 module consisting of 36 polycrystalline silicon cells in series (under a  $1000 \text{ W/m}^2$  at  $45 \text{ }^\circ\text{C}$ ). These two data sets of experimental I-V data have been widely used as the benchmark datasets to test and compare the performance of diverse methods [1,2,4,11,31,32,34] developed for parameter estimation of SDM, DDM and PMM. And then, in addition to the benchmark datasets, the real datasets of two recent reported PV panels are also chosen to further establish the ability of proposed ImCSA for parameter estimation under a real implementation. The real datasets of PV panels are gotten from [45], where the experimental I-V data of two PV panels, namely, polycrystalline STP6-120/36 panel and monocrystalline STM6-40/36 panel are measured by setting up a simple load scanning experiment. Both PV panels consist of 36 cells in series, while operating at  $55 \text{ }^\circ\text{C}$  and  $51 \text{ }^\circ\text{C}$ , respectively.

All the programs are executed using MATLAB in a computer with an Intel(R) Core(TM) i5-2415M @ 2.30 GHz CPU processor, 4 GB RAM and Windows 7 system. The parameters for the original CSA are set as follows: the population size  $n = 25$ , the fraction probability  $P_a = 0.25$ , the step size scaling factor  $\alpha = 0.01$ , the distribution factor  $\beta = 1.5$ . For the proposed ImCSA, the parameters are given by: the population size  $n = 25$ , the maximum and minimum fraction probability  $P_{a,\max}$  and  $P_{a,\min}$  are 0.25 and 0.01 respectively. The maximum number of iterations  $It_{\max}$  is set to 1500 for SDM, 8000 for DDM and 1000 for PMM. In addition, all experiments are performed for 30 independent runs and the best result is presented at each case.

### 5.1. Results on Benchmark Datasets

#### 5.1.1. Case Study 1: Single Diode Model

In this case, there are five unknown parameters that need to be estimated for the SDM. The range of each parameter used in the literature [1,2,4,11,24] are set as follows:  $I_{ph} \text{ (A)} \in [0, 1]$ ,  $I_{sd} \text{ (}\mu\text{A)} \in [0, 1]$ ,  $a \in [1, 2]$ ,  $R_s \text{ (}\Omega) \in [0, 0.5]$ ,  $R_{sh} \text{ (}\Omega) \in [0, 100]$ . The experimental data measured from RTC France silicon solar cell at  $33 \text{ }^\circ\text{C}$  contain 26 pairs of voltage and current values used the same as in the literature [1,2,4,11,14,24]. These data are cited to obtain the optimal parameters vector  $\theta$  for the SDM of RTC France silicon solar cell by the proposed ImCSA.

Table 1 tabulates the statistics of the OF (RMSE) values for the SDM of RTC France silicon solar cell computed using the ImCSA and CSA. Table 1 shows that the ImCSA performs better than CSA in all terms of the best, mean, median, worst and standard deviation (Std) of the OF (RMSE) values in all 30 independent runs. Moreover, the best OF (RMSE) value quantifies the best accuracy, the mean OF (RMSE) value quantifies the average accuracy, and the standard deviation (Std) of the OF (RMSE) value indicates the reliability of the parameter estimation methods, respectively. From Table 1 it can be found that the ImCSA achieves the best, mean, median, and worst of the OF (RMSE) values as low as  $9.860219 \times 10^{-4}$ . Especially, the ImCSA obtains a Std of  $2.987589 \times 10^{-12}$ , which is obviously far better than that calculated by CSA as shown in Table 1. These results indicate that the proposed ImCSA really enhances the performance of original CSA and is more accurate and reliable than CSA. Furthermore, the convergence performance for the best run of the proposed ImCSA for parameter estimation of the SDM of RTC France silicon solar cell is represented in Figure 4. It can be seen from Figure 4 that the ImCSA fastly converges to a comparatively stable OF value in less than 300 iterations.

**Table 1.** Statistics of the OF (RMSE) values for the SDM of RTC France silicon solar cell using the proposed ImCSA and CSA.

Algorithm	OF (RMSE)				
	Best	Mean	Median	Worst	Std
ImCSA	$9.860219 \times 10^{-4}$	$9.860219 \times 10^{-4}$	$9.860219 \times 10^{-4}$	$9.860219 \times 10^{-4}$	$2.987589 \times 10^{-12}$
CSA	$9.860227 \times 10^{-4}$	$9.894848 \times 10^{-4}$	$9.865435 \times 10^{-4}$	$1.031010 \times 10^{-3}$	$8.570571 \times 10^{-6}$

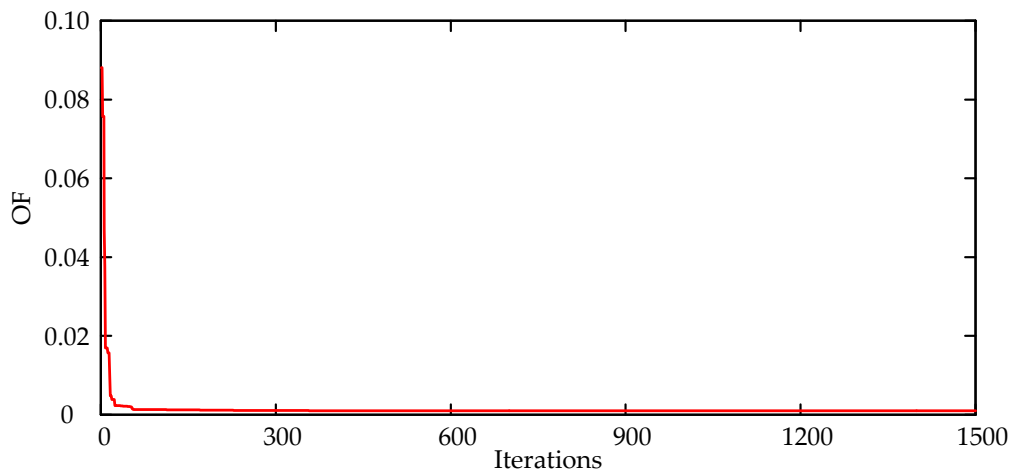
**Figure 4.** Convergence characteristic of the proposed ImCSA for parameter estimation of the SDM of RTC France silicon solar cell.

Table 2 summarizes the optimal parameters such as  $I_{ph}$ ,  $I_{sd}$ ,  $a$ ,  $R_s$ ,  $R_{sh}$  values and the corresponding objective value of OF (RMSE) for the SDM achieved by the ImCSA compared with those by CSA and several other parameter estimation methods such as TLABC [34], CIABC [11], MSSO [33], IJAYA [32], SATLBO [31], GOTLBO [10], EHA-NMS [30], CARO [4], IABC [29], MABC [28], ABC [2], BBO-M [27],  $R_{cr}$ -IJADE [25], ABSO [24], HS [1], PS [21], CPSO [20], and GA [1]. These approaches are selected for comparison here due to their good performance in estimating parameters for the SDM of the PV cell reported in the recent literature. From the OF (RMSE) values in Table 2, it is apparent that the proposed ImCSA, together with the TLABC, CIABC, SATLBO, EHA-NMS, and  $R_{cr}$ -IJADE obtain the best OF (RMSE) value ( $9.8602 \times 10^{-4}$ ), and CSA gets the second best OF (RMSE) value ( $9.86023 \times 10^{-4}$ ), followed by IJAYA, MSSO, MABC, ABC, BBO-M, CARO, GOTLBO, ABSO, HS, IABC, CPSO, PS and GA, which indicates that the proposed ImCSA improves the performance of the original CSA. Consequently, the optimal parameters values sought out via the proposed ImCSA are closer to the real ones for the SDM of the solar cell, thus the parameters estimated by ImCSA are accurate.

To make a further investigation on the quality of the parameters estimated by the proposed ImCSA, these estimated parameters values of  $I_{ph}$ ,  $I_{sd}$ ,  $a$ ,  $R_s$  and  $R_{sh}$  are put into the SDM in Equation (4) to reconstruct the calculated current data and calculated power data at experimental voltage point. The experimental data (voltage and current), the calculated data and the individual absolute error (IAE) between experimental and calculated data are listed in Table 3. Table 3 (columns 5 and 7) and the last line of Table 3 show that both the IAE and their sum are so small, which gives concrete evidence that the parameter values estimated by the ImCSA are very precise. The I-V and P-V (power versus voltage) characteristics of the best model parameters estimated by the ImCSA and the experimental data are illustrated in Figure 5. Figure 5 shows that the calculated data of SDM are in excellent accordance with the experimental data almost in all data points, which further demonstrates the optimal parameters values estimated by the ImCSA are very precise.

**Table 2.** Comparison among various parameter estimation algorithms for the SDM of RTC France silicon solar cell.

Algorithm	$I_{ph}$ (A)	$I_{sd}$ ( $\mu$ A)	$a$	$R_s$ ( $\Omega$ )	$R_{sh}$ ( $\Omega$ )	OF (RMSE)
ImCSA	0.760776	0.323021	1.481718	0.036377	53.718524	$9.8602 \times 10^{-4}$
CSA	0.760776	0.322821	1.481656	0.036380	53.696699	$9.86023 \times 10^{-4}$
TLABC [34]	0.76078	0.32302	1.48118	0.03638	53.71636	$9.8602 \times 10^{-4}$
CIABC [11]	0.760776	0.32302	1.48102	0.036377	53.71867	$9.8602 \times 10^{-4}$
MSSO [33]	0.760777	0.323564	1.481244	0.036370	53.742465	$9.8607 \times 10^{-4}$
IJAYA [32]	0.7608	0.3228	1.4811	0.0364	53.7595	$9.8603 \times 10^{-4}$
SATLBO [31]	0.7608	0.32315	1.48123	0.03638	53.7256	$9.8602 \times 10^{-4}$
GOTLBO [10]	0.760780	0.331552	1.483820	0.036265	54.115426	$9.87442 \times 10^{-4}$
EHA-NMS [30]	0.760776	0.323021	1.481184	0.036377	53.718521	$9.8602 \times 10^{-4}$
CARO [4]	0.76079	0.31724	1.48168	0.03644	53.0893	$9.8665 \times 10^{-4}$
IABC [29]	0.7599	0.33243	1.4842	0.0363	54.4610	$10.000 \times 10^{-4}$
MABC [28]	0.760779	0.321323	1.481385	0.036389	53.39999	$9.861 \times 10^{-4}$
ABC [2]	0.7608	0.3251	1.4817	0.0364	53.6433	$9.862 \times 10^{-4}$
BBO-M [27]	0.76078	0.31874	1.47984	0.03642	53.36227	$9.8634 \times 10^{-4}$
$R_{cr}$ -IJADE [25]	0.760776	0.323021	1.481184	0.036377	53.718526	$9.8602 \times 10^{-4}$
ABSO [24]	0.76080	0.30623	1.47583	0.03659	52.2903	$9.9124 \times 10^{-4}$
HS [1]	0.76070	0.30495	1.47538	0.03663	53.5946	$9.9510 \times 10^{-4}$
PS [21]	0.7617	0.9980	1.6000	0.0313	64.1026	$14.94 \times 10^{-3}$
CPSO [20]	0.7607	0.4000	1.5033	0.0354	59.012	$1.39 \times 10^{-3}$
GA [1]	0.7619	0.8087	1.5751	0.0299	42.3729	$19.08 \times 10^{-3}$

**Table 3.** The calculated results of the proposed ImCSA for the SDM of RTC France silicon solar cell.

Item	Experimental Data		Calculated Current Data		Calculated Power Data	
	V (V)	I (A)	$I_{cal}$ (A)	IAE	$P_{cal}$ (W)	IAE
1	-0.2057	0.7640	0.76408764	0.00008764	-0.15717283	0.00001803
2	-0.1291	0.7620	0.76266264	0.00066264	-0.09845975	0.00008555
3	-0.0588	0.7605	0.76135473	0.00085473	-0.04476766	0.00005026
4	0.0057	0.7605	0.76015423	0.00034577	0.00433288	0.00000197
5	0.0646	0.7600	0.75905585	0.00094415	0.04903501	0.00006099
6	0.1185	0.7590	0.75804301	0.00095699	0.08982810	0.00011340
7	0.1678	0.7570	0.75709159	0.00009159	0.12703997	0.00001537
8	0.2132	0.7570	0.75614207	0.00085793	0.16120949	0.00018291
9	0.2545	0.7555	0.75508732	0.00041268	0.19216972	0.00010503
10	0.2924	0.7540	0.75366447	0.00033553	0.22037149	0.00009811
11	0.3269	0.7505	0.75138806	0.00088806	0.24562876	0.00029031
12	0.3585	0.7465	0.74734834	0.00084834	0.26792438	0.00030413
13	0.3873	0.7385	0.74009688	0.00159688	0.28663952	0.00061847
14	0.4137	0.7280	0.72739678	0.00060322	0.30092405	0.00024955
15	0.4373	0.7065	0.70695327	0.00045327	0.30915067	0.00019822
16	0.4590	0.6755	0.67529489	0.00020511	0.30996036	0.00009414
17	0.4784	0.6320	0.63088431	0.00111569	0.30181505	0.00053375
18	0.4960	0.5730	0.57208207	0.00091793	0.28375271	0.00045529
19	0.5119	0.4990	0.49949164	0.00049164	0.25568977	0.00025167
20	0.5265	0.4130	0.41349356	0.00049356	0.21770436	0.00025986
21	0.5398	0.3165	0.31721950	0.00071950	0.17123509	0.00038839
22	0.5521	0.2120	0.21210317	0.00010317	0.11710216	0.00005696
23	0.5633	0.1035	0.10272135	0.00077865	0.05786294	0.00043861
24	0.5736	-0.0100	-0.00924885	0.00075115	-0.00530514	0.00043086
25	0.5833	-0.1230	-0.12438136	0.00138136	-0.07255165	0.00080575
26	0.5900	-0.2100	-0.20919308	0.00080692	-0.12342392	0.00047608
Sum of IAE				0.01770412		0.00658366

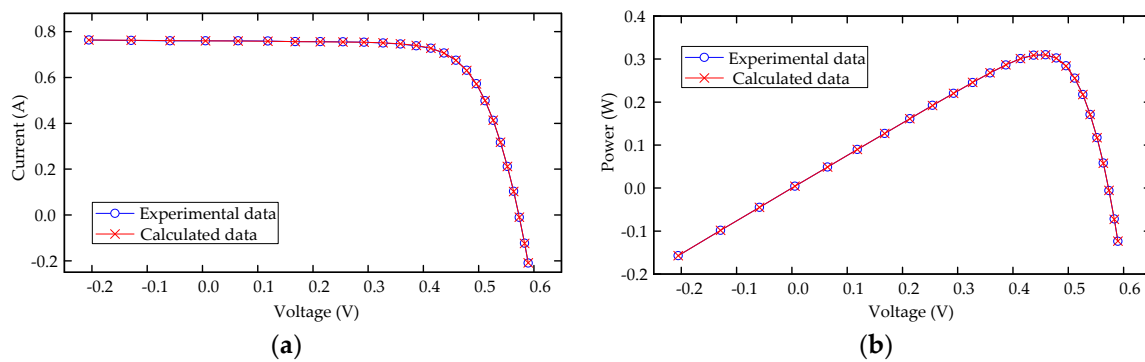


**Figure 5.** Comparisons between the experimental data and calculated data obtained by the proposed ImCSA for the SDM of RTC France silicon solar cell: (a) I-V characteristics; (b) P-V characteristics.

### 5.1.2. Case Study 2: Double Diode Model

For the DDM in this case, seven unknown parameters need to be estimated. The range of each parameter reported in the literature [1,2,4,11,24] are set as follows:  $I_{ph}$  (A)  $\in [0, 1]$ ,  $I_{sd1}$  ( $\mu$ A)  $\in [0, 1]$ ,  $I_{sd2}$  ( $\mu$ A)  $\in [0, 1]$ ,  $a_1 \in [1, 2]$ ,  $a_2 \in [1, 2]$ ,  $R_s$  ( $\Omega$ )  $\in [0, 0.5]$ ,  $R_{sh}$  ( $\Omega$ )  $\in [0, 100]$ . The 26 pairs of voltage and current values measured from RTC France silicon solar cell at 33 °C are the same as in Table 3 (columns 2 and 3) from case study 1. Here, the proposed ImCSA is employed to estimate the optimal parameters vector  $\theta$  for the DDM of the RTC France silicon solar cell.

Table 4 shows the statistics of the OF (RMSE) values for the DDM of RTC France silicon solar cell obtained by the ImCSA and CSA. Table 4 clearly shows that the ImCSA presents better statistics when compared with CSA. The ImCSA achieves a best OF (RMSE) value of  $9.8249 \times 10^{-4}$ , which is apparently better than the best OF (RMSE) value achieved by CSA as shown in Table 4. The proposed ImCSA outperforms original CSA in all terms of the best, mean, median, worst and Std of the OF (RMSE) values over 30 independent runs. Moreover, the ImCSA obtains a good Std of  $2.8197 \times 10^{-7}$  while CSA obtains a Std of  $4.1755 \times 10^{-6}$  as presented in Table 4. These results imply that the proposed ImCSA remarkably enhances the performance of original CSA and is better than original CSA in terms of accuracy and reliability since the best OF (RMSE) value quantifies the best accuracy and the Std of the OF (RMSE) value implies the reliability of parameter estimation methods as aforementioned. In addition, the convergence performance for the best run of the ImCSA for parameter estimation of the DDM of RTC France silicon solar cell is shown in Figure 6. It can be observed from Figure 6 that the objective value becomes relatively stable in less than 1000 iterations.

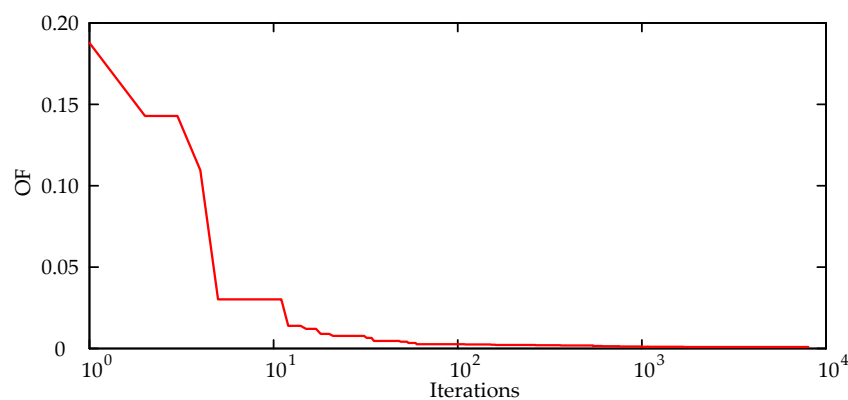


**Figure 6.** Convergence characteristic of the proposed ImCSA for parameter estimation of the DDM of RTC France silicon solar cell.

**Table 4.** Statistics of the OF (RMSE) values for the DDM of RTC France silicon solar cell using the proposed ImCSA and CSA.

Algorithm	OF (RMSE)				
	Best	Mean	Median	Worst	Std
ImCSA	$9.8249 \times 10^{-4}$	$9.8258 \times 10^{-4}$	$9.8249 \times 10^{-4}$	$9.8396 \times 10^{-4}$	$2.8197 \times 10^{-7}$
CSA	$9.8292 \times 10^{-4}$	$9.8626 \times 10^{-4}$	$9.8535 \times 10^{-4}$	$1.0056 \times 10^{-3}$	$4.1755 \times 10^{-6}$

Table 5 illustrates the optimal parameters such as  $I_{ph}$ ,  $I_{sd1}$ ,  $I_{sd2}$ ,  $a_1$ ,  $a_2$ ,  $R_s$ ,  $R_{sh}$  values and the corresponding objective value of OF (RMSE) for the DDM estimated by the ImCSA compared with those by CSA and several other reported parameter estimation methods such as TLABC [34], CIABC [11], MSSO [33], IJAYA [32], SATLBO [31], GOTLBO [10], EHA-NMS [30], CARO [4], IABC [29], MABC [28], ABC [2], BBO-M [27],  $R_{cr}$ -IJADE [25], ABSO [24], HS [1], and PS [21]. From the OF (RMSE) values in Table 5, the EHA-NMS and  $R_{cr}$ -IJADE provide the best OF (RMSE) value ( $9.8248 \times 10^{-4}$ ). The ImCSA achieves the second best OF (RMSE) value ( $9.8249 \times 10^{-4}$ ), which is very close to that of EHA-NMS and  $R_{cr}$ -IJADE. The other approaches are ranked as CARO, CIABC, BBO-M, MABC, SATLBO, MSSO, CSA, IJAYA, GOTLBO, ABSO, TLABC, ABC, IABC, HS, and PS. These results imply that the proposed ImCSA considerably improves the performance of the original CSA. Consequently, the optimal parameters values determined by the ImCSA are more close to the real ones for the DDM of the PV cell.

To further establish the quality of the parameters estimated by the ImCSA, seven estimated parameters values of  $I_{ph}$ ,  $I_{sd1}$ ,  $I_{sd2}$ ,  $a_1$ ,  $a_2$ ,  $R_s$  and  $R_{sh}$  are put into Equation (8) to reconstruct the calculated data of DDM of the RTC France silicon solar cell. The calculated data and the experimental data are compared in Table 6 for observation on the accordance between them, and the IAE between experimental and calculated data are also presented in Table 6. It can be seen from Table 6 (columns 5 and 7) and the last line of Table 6 that both the IAE and their sum are negligible small and the computed data of DDM are remarkably consistent with the experimental data. Moreover, Figure 7 plots the I-V and P-V characteristics of the best model parameters identified by the proposed ImCSA and the experimental data. It is clear from Figure 7 that the computed data are in good agreement with the experimental data. Cross checking Tables 3 and 5, Figures 6 and 7, we can see that the sum of IAE of DDM are smaller than those of SDM, which further validates the optimal parameter values estimated by ImCSA are very precise.

**Table 5.** Comparison among various parameter estimation algorithms for the DDM of RTC France silicon solar cell.

Algorithm	$I_{ph}$ (A)	$I_{sd1}$ ( $\mu$ A)	$I_{sd2}$ ( $\mu$ A)	$a_1$	$a_2$	$R_s$ ( $\Omega$ )	$R_{sh}$ ( $\Omega$ )	OF (RMSE)
ImCSA	0.760781	0.225966	0.747309	1.451543	2.000000	0.036740	55.482685	$9.8249 \times 10^{-4}$
CSA	0.760772	0.503010	0.255099	1.999954	1.461682	0.036620	54.890635	$9.8292 \times 10^{-4}$
TLABC [34]	0.76081	0.42394	0.24011	1.9075	1.45671	0.03667	54.66797	$9.8414 \times 10^{-4}$
CIABC [11]	0.760781	0.227828	0.647650	1.451623	1.988343	0.036728	55.378261	$9.8262 \times 10^{-4}$
MSSO [33]	0.760748	0.234925	0.671593	1.454255	1.995305	0.036688	55.714662	$9.8281 \times 10^{-4}$
IJAYA [32]	0.7601	0.0050445	0.75094	1.2186	1.6247	0.0376	77.8519	$9.8293 \times 10^{-4}$
SATLBO [31]	0.76078	0.25093	0.545418	1.45982	1.99941	0.03663	55.1170	$9.82804 \times 10^{-4}$
GOTLBO [10]	0.760752	0.800195	0.220462	1.999973	1.448974	0.036783	56.075304	$9.83177 \times 10^{-4}$
EHA-NMS [30]	0.760781	0.225974	0.749346	1.451017	2.000000	0.036740	55.485441	$9.8248 \times 10^{-4}$
CARO [4]	0.76075	0.29315	0.09098	1.47338	1.77321	0.03641	54.3967	$9.8260 \times 10^{-4}$
IABC [29]	0.7609	0.26900	0.28198	1.4670	1.8722	0.0364	55.2307	$10.000 \times 10^{-4}$
MABC [28]	0.76078	0.63069	0.241029	2.000005	1.45685	0.036712	54.75500	$9.8276 \times 10^{-4}$
ABC [2]	0.7608	0.0407	0.2874	1.4495	1.4885	0.0364	53.7804	$9.861 \times 10^{-4}$
BBO-M [27]	0.76083	0.59115	0.24523	2.00000	1.45798	0.03664	55.0494	$9.8272 \times 10^{-4}$
$R_{cr}$ -IJADE [25]	0.760781	0.225974	0.749347	1.451017	2.000000	0.036740	55.485443	$9.8248 \times 10^{-4}$
ABSO [24]	0.76078	0.26713	0.38191	1.46512	1.98152	0.03657	54.6219	$9.8344 \times 10^{-4}$
HS [1]	0.76176	0.12545	0.25470	1.49439	1.49989	0.03545	46.82696	$1.26 \times 10^{-3}$
PS [21]	0.7602	0.9889	0.0001	1.6000	1.1920	0.0320	81.3008	$15.18 \times 10^{-3}$

**Table 6.** The calculated results of the proposed ImCSA for the DDM of RTC France silicon solar cell.

Item	Experimental Data		Calculated Current Data		Calculated Power Data	
	V (V)	I (A)	$I_{cal}$ (A)	IAE	$P_{cal}$ (W)	IAE
1	-0.2057	0.7640	0.76398357	0.00001643	-0.15715142	0.00000338
2	-0.1291	0.7620	0.76260378	0.00060378	-0.09845215	0.00007795
3	-0.0588	0.7605	0.76133716	0.00083716	-0.04476663	0.00004923
4	0.0057	0.7605	0.76017397	0.00032603	0.00433299	0.00000186
5	0.0646	0.7600	0.75910819	0.00089181	0.04903839	0.00005761
6	0.1185	0.7590	0.75812190	0.00087810	0.08983745	0.00010405
7	0.1678	0.7570	0.75718834	0.00018834	0.12705620	0.00003160
8	0.2132	0.7570	0.75624409	0.00075591	0.16123124	0.00016116
9	0.2545	0.7555	0.75517755	0.00032245	0.19219269	0.00008206
10	0.2924	0.7540	0.75372279	0.00027721	0.22038854	0.00008106
11	0.3269	0.7505	0.75139612	0.00089612	0.24563139	0.00029294
12	0.3585	0.7465	0.74729625	0.00079625	0.26790571	0.00028546
13	0.3873	0.7385	0.73999153	0.00149153	0.28659872	0.00057767
14	0.4137	0.7280	0.72726505	0.00073495	0.30086955	0.00030405
15	0.4373	0.7065	0.70683595	0.00033595	0.30909936	0.00014691
16	0.4590	0.6755	0.67523018	0.00026982	0.30993065	0.00012385
17	0.4784	0.6320	0.63088762	0.00111238	0.30181664	0.00053216
18	0.4960	0.5730	0.57214020	0.00085980	0.28378154	0.00042646
19	0.5119	0.4990	0.49957049	0.00057049	0.25573014	0.00029204
20	0.5265	0.4130	0.41355625	0.00055625	0.21773737	0.00029287
21	0.5398	0.3165	0.31724205	0.00074205	0.17124726	0.00040056
22	0.5521	0.2120	0.21208151	0.00008151	0.11709020	0.00004500
23	0.5633	0.1035	0.10267162	0.00082838	0.05783492	0.00046663
24	0.5736	-0.0100	-0.00929718	0.00070282	-0.00533286	0.00040314
25	0.5833	-0.1230	-0.12439038	0.00139038	-0.07255691	0.00081101
26	0.5900	-0.2100	-0.20914698	0.00085302	-0.12339672	0.00050328
Sum of IAE				0.01731892		0.00655397

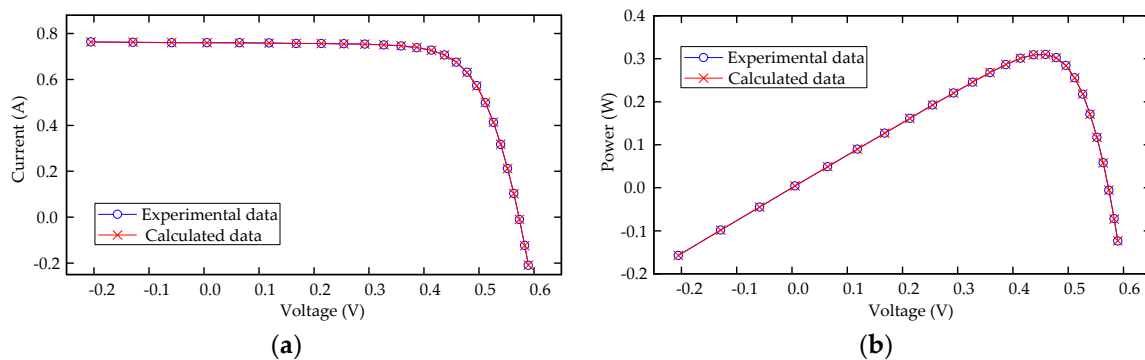


**Figure 7.** Comparisons between the experimental data and calculated data obtained by the proposed ImCSA for the DDM of RTC France silicon solar cell: (a) I-V characteristics; (b) P-V characteristics.

### 5.1.3. Case Study 3: PV Module Model

In this case, there are five unknown parameters that need to be estimated for the PMM. The range of each parameter used in the literature [4,30–32,34] are set as follows:  $I_{phm}$  (A)  $\in [0, 2]$ ,  $I_{sdm}$  ( $\mu$ A)  $\in [0, 50]$ ,  $a_m \in [1, 50]$ ,  $R_{sm}$  ( $\Omega$ )  $\in [0, 2]$ ,  $R_{sh_m}$  ( $\Omega$ )  $\in [0, 2000]$ . The experimental data measured from Photowatt-PWP201 module at 45 °C contain 25 pairs of voltage and current values reported in the literature [4,14,31,32,34]. These data are cited to find the optimal parameters vector  $\theta$  for the PMM of Photowatt-PWP201 module by the proposed ImCSA. The statistics of the OF (RMSE) values for the PMM of Photowatt-PWP201 module achieved by the ImCSA and CSA are displayed in Table 7. As can be seen in this table, the ImCSA performs better than CSA in terms of all statistical indicators, including the best, mean, median, worst and Std of the OF (RMSE) values over 30 runs. Additionally, the ImCSA achieves the best, mean, and median of the OF (RMSE) values as low as  $2.425075 \times 10^{-3}$

as shown in Table 7. Particularly, it can be observed from Table 7 that the ImCSA obtains a Std of  $2.915426 \times 10^{-9}$ , which is clearly far better than that calculated by CSA. Similar to previous cases, these results prove that the proposed ImCSA is indeed still more accurate and reliable than original CSA and improves the performance of CSA. Furthermore, the convergence performance for the best run of the proposed ImCSA for parameter estimation of the PMM of the Photowatt-PWP201 module is given in Figure 8. It can be found from Figure 8 that the ImCSA rapidly converges to a comparatively stable objective value in less than 100 iterations.

**Table 7.** Statistics of the OF (RMSE) values for the PMM of Photowatt-PWP201 module using the proposed ImCSA and CSA.

Algorithm	OF (RMSE)				
	Best	Mean	Median	Worst	Std
ImCSA	$2.425075 \times 10^{-3}$	$2.425075 \times 10^{-3}$	$2.425075 \times 10^{-3}$	$2.425091 \times 10^{-3}$	$2.915426 \times 10^{-3}$
CSA	$2.425082 \times 10^{-3}$	$2.430857 \times 10^{-3}$	$2.426771 \times 10^{-3}$	$2.499628 \times 10^{-3}$	$1.418512 \times 10^{-5}$

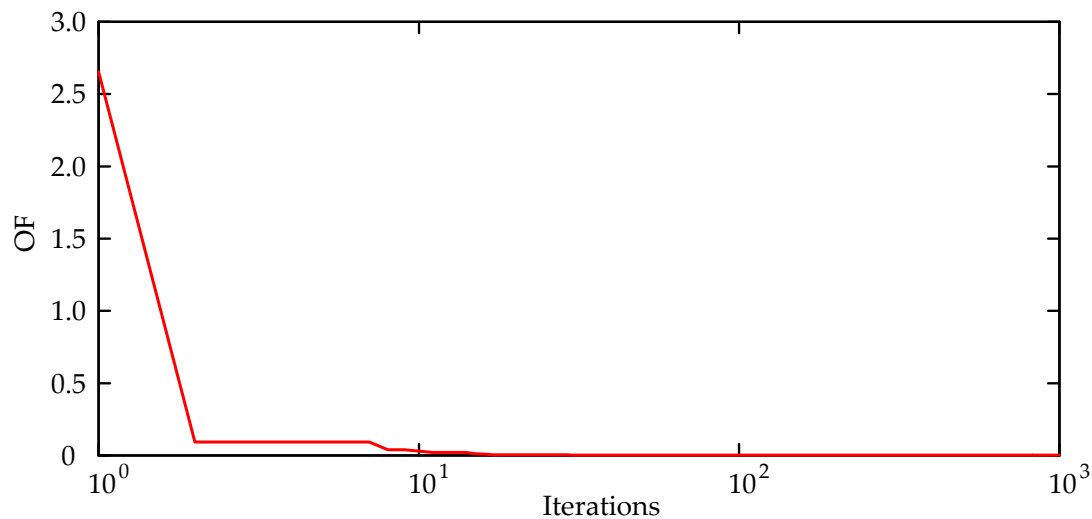


**Figure 8.** Convergence characteristic of the proposed ImCSA for parameter estimation of the PMM of Photowatt-PWP201 module.

Table 8 shows the optimal parameters such as  $I_{phm}$ ,  $I_{sdm}$ ,  $a_m$ ,  $R_{sm}$ ,  $R_{shm}$  values and the corresponding objective value of OF (RMSE) for the PMM obtained by the ImCSA in comparisons with those by CSA and some other parameter estimation methods such as TLABC [34], IJAYA [32], SATLBO [31], EHA-NMS [30], CARO [4], MPCOA [26],  $R_{cr}$ -IJADE [25], SA [23], PS [21], and CPSO [20]. It is obvious from the OF (RMSE) values in Table 8 that the proposed ImCSA, TLABC, IJAYA, SATLBO, EHA-NMS, MPCOA, and  $R_{cr}$ -IJADE acquire the lowest OF (RMSE) value ( $2.425 \times 10^{-3}$ ), followed by CSA, CARO, SA, CPSO, and PS, which indicates that the proposed ImCSA evidently enhances the performance of the original CSA and the optimal parameters values sought out via the ImCSA are closer to the real ones for the PMM of the PV module.

**Table 8.** Comparison among various parameter estimation algorithms for the PMM of Photowatt-PWP201 module.

Algorithm	$I_{phm}$ (A)	$I_{sdm}$ ( $\mu$ A)	$a_m$	$R_{sm}$ ( $\Omega$ )	$R_{shm}$ ( $\Omega$ )	OF (RMSE)
ImCSA	1.030514	3.482263	48.660397	1.201271	981.982233	$2.425 \times 10^{-3}$
CSA	1.030496	3.485411	48.663834	1.201201	984.320163	$2.42508 \times 10^{-3}$
TLABC [34]	1.03056	3.4715	48.63131	1.20165	972.93567	$2.425 \times 10^{-3}$
IJAYA [32]	1.0305	3.4703	48.6298	1.2016	977.3752	$2.425 \times 10^{-3}$
SATLBO [31]	1.030511	3.48271	48.6433077	1.201263	982.40376	$2.425 \times 10^{-3}$
EHA-NMS [30]	1.030514	3.482263	48.642835	1.201271	981.982256	$2.425 \times 10^{-3}$
CARO [4]	1.03185	3.28401	48.4.363	1.20556	841.3213	$2.427 \times 10^{-3}$
MPCOA [26]	1.03188	3.37370	48.50646	1.20295	849.6927	$2.425 \times 10^{-3}$
$R_{cr}$ -IJADE [25]	1.030514	3.482263	48.642835	1.201271	981.982240	$2.425 \times 10^{-3}$
SA [23]	1.0331	3.6642	48.8211	1.1989	833.3333	$2.7 \times 10^{-3}$
PS [21]	1.0313	3.1756	48.2889	1.2053	714.2857	$1.18 \times 10^{-2}$
CPSO [20]	1.0286	8.3010	52.2430	1.0755	1850.1000	$3.5 \times 10^{-3}$

Just like before, for further investigating the quality of the parameters identified by the proposed ImCSA, these identified parameters values of  $I_{phm}$ ,  $I_{sdm}$ ,  $a_m$ ,  $R_{sm}$  and  $R_{shm}$  are returned to Equation (10) to rebuild the calculated current data and calculated power data at experimental voltage point. Table 9 tabulates the calculated results. From Table 9 (columns 5 and 7) and the last line of Table 9, both the  $IAE$  and their sum are very tiny, which provides a concrete proof of the ImCSA in accurately estimating the parameters. The I-V and P-V characteristics of the best model parameters estimated by the ImCSA and the experimental data are shown in Figure 9, it can be seen from Figure 9 that the calculated data of PMM match the experimental data nicely, which further demonstrates the high accuracy parameters are achieved again by the proposed ImCSA.

**Table 9.** The calculated results of the proposed ImCSA for the PMM of Photowatt-PWP201 module.

Item	Experimental Data		Calculated Current Data		Calculated Power Data	
	V (V)	I (A)	$I_{cal}$ (A)	$IAE$	$P_{cal}$ (W)	$IAE$
1	0.1248	1.0315	1.02912209	0.00237791	0.12843444	0.00029676
2	1.8093	1.0300	1.02738435	0.00261565	1.85884651	0.00473249
3	3.3511	1.0260	1.02574214	0.00025786	3.43736448	0.00086412
4	4.7622	1.0220	1.02410399	0.00210399	4.87698803	0.01001963
5	6.0538	1.0180	1.02228341	0.00428341	6.18869931	0.02593091
6	7.2364	1.0155	1.01991740	0.00441740	7.38053027	0.03196607
7	8.3189	1.0140	1.01635081	0.00235081	8.45492077	0.01955617
8	9.3097	1.0100	1.01049143	0.00049143	9.40737206	0.00457506
9	10.2163	1.0035	1.00067876	0.00282124	10.22323441	0.02882264
10	11.0449	0.9880	0.98465335	0.00334665	10.87539777	0.03696343
11	11.8018	0.9630	0.95969741	0.00330259	11.32615687	0.03897653
12	12.4929	0.9255	0.92304875	0.00245125	11.53155579	0.03062316
13	13.1231	0.8725	0.87258816	0.00008816	11.45106168	0.00115693
14	13.6983	0.8075	0.80731012	0.00018988	11.05877623	0.00260102
15	14.2221	0.7265	0.72795782	0.00145782	10.35308888	0.02073323
16	14.6995	0.6345	0.63646618	0.00196618	9.35573459	0.02890184
17	15.1346	0.5345	0.53569607	0.00119607	8.10754576	0.01810206
18	15.5311	0.4275	0.42881615	0.00131615	6.65998648	0.02044123
19	15.8929	0.3185	0.31866866	0.00016866	5.06456910	0.00268045
20	16.2229	0.2085	0.20785711	0.00064289	3.37204517	0.01042948
21	16.5241	0.1010	0.09835421	0.00264579	1.62521481	0.04371929
22	16.7987	-0.0080	-0.00816934	0.00016934	-0.13723426	0.00284466
23	17.0499	-0.1110	-0.11096846	0.00003154	-1.89200116	0.00053774
24	17.2793	-0.2090	-0.20911762	0.00011762	-3.61340604	0.00203234
25	17.4885	-0.3030	-0.30202238	0.00097762	-5.28191833	0.01709717
Sum of $IAE$				0.04178790		0.40460442

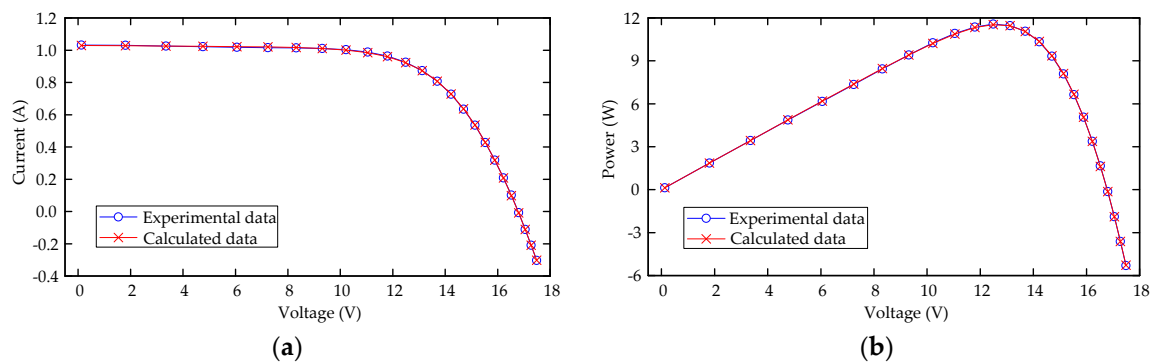


**Figure 9.** Comparisons between the experimental data and calculated data obtained by the proposed ImCSA for the PMM of Photowatt-PWP201 module: (a) I-V characteristics; (b) P-V characteristics.

## 5.2. Results on Real Datasets of PV Panels

### 5.2.1. Case Study 1: PV Module Model with Real Dataset of a Polycrystalline Panel

This subsection is to investigate the performance of proposed ImCSA for parameter estimation under a real implementation. A real dataset is considered, where the experimental I–V data from a polycrystalline STP6-120/36 panel at 55 °C [45] contain 22 pairs of voltage and current values. This PV panel consists of 36 polycrystalline cells in series and size of each cell is 156 mm × 156 mm.  $V_{OC} = 19.21$  V,  $I_{SC} = 7.48$  A,  $V_M = 14.93$  V, and  $I_M = 6.83$  A. In this case, there are five unknown parameters needed to be estimated for the PMM of polycrystalline STP6-120/36 panel. The range of each parameter are set as follows:  $I_{ph}$  (A)  $\in [0, 10]$ ,  $I_{sd}$  ( $\mu$ A)  $\in [1, 2]$ ,  $a \in [1, 2]$ ,  $R_s$  (m $\Omega$ )  $\in [0, 10]$ ,  $R_{sh}$  ( $\Omega$ )  $\in [0, 10]$ . The experimental I–V data are applied for finding optimal parameters vector  $\theta$  for the PMM of STP6-120/36 panel by the proposed ImCSA.

Table 10 shows the statistics of the OF (RMSE) values for the PMM of polycrystalline STP6-120/36 panel obtained by the ImCSA and CSA. Evidently, Table 10 shows that all terms of the best, mean, median, worst and Std of the OF (RMSE) values over 30 runs obtained by the ImCSA are smaller than those calculated by CSA. Furthermore, it can be found from Table 10 that the ImCSA provides the best, mean, median, and worst of the OF (RMSE) values as low as  $1.5865799 \times 10^{-2}$ . In particular, the ImCSA obtains a Std of  $4.6901709 \times 10^{-15}$ , which is obviously far lower than that calculated by CSA as shown in Table 10. These results give concrete evidence that the ImCSA improves the performance of original CSA and is more accurate and reliable than CSA. In addition, Figure 10 displays the convergence performance for the best run of the ImCSA for parameter estimation of the PMM of polycrystalline STP6-120/36 panel. It can be seen from this figure that the ImCSA can attain a relatively stable OF value in less than 100 iterations, which implies its fast convergence.

**Table 10.** Statistics of the OF (RMSE) values for the PMM of polycrystalline STP6-120/36 panel using the proposed ImCSA and CSA.

Algorithm	OF (RMSE)				
	Best	Mean	Median	Worst	Std
ImCSA	$1.5865799 \times 10^{-2}$	$1.5865799 \times 10^{-2}$	$1.5865799 \times 10^{-2}$	$1.5865799 \times 10^{-2}$	$4.6901709 \times 10^{-15}$
CSA	$1.5865806 \times 10^{-2}$	$1.5869596 \times 10^{-2}$	$1.5866453 \times 10^{-2}$	$1.5892796 \times 10^{-2}$	$6.2673061 \times 10^{-6}$

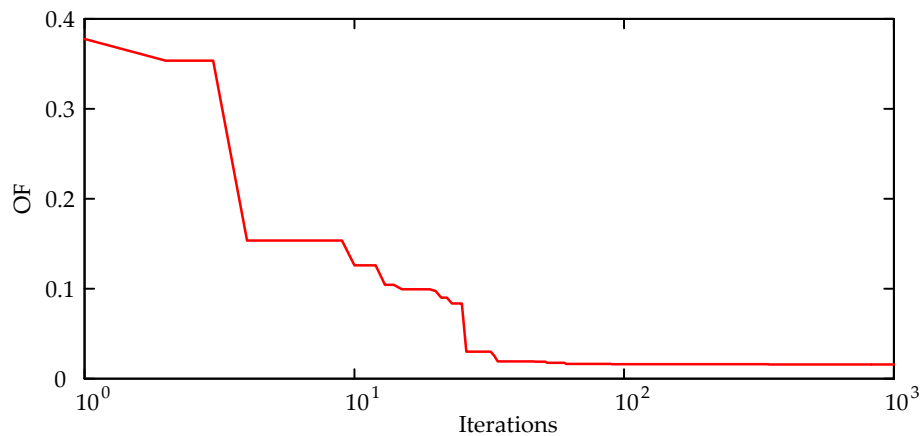


**Figure 10.** Convergence characteristic of the proposed ImCSA for parameter estimation of the PMM of polycrystalline STP6-120/36 panel.

Table 11 illustrates the optimal parameters values and the corresponding objective value of OF (RMSE) for the PMM of polycrystalline STP6-120/36 panel achieved by the ImCSA compared with those by CSA and several other recent parameter estimation methods such as ABC [11], CIABC [11], and Reference [45]. It is obvious from the OF (RMSE) values in Table 11 that the proposed ImCSA obtains the lowest OF (RMSE) value among these methods, followed by CSA, CIABC, Reference [45], and ABC, which implies that the proposed ImCSA enhances the performance of original CSA and outperforms all other algorithms. Consequently, the optimal parameters values found by the proposed ImCSA are closer to the real ones for the PMM of polycrystalline STP6-120/36 panel, whereby the proposed ImCSA achieves the high accuracy parameter values.

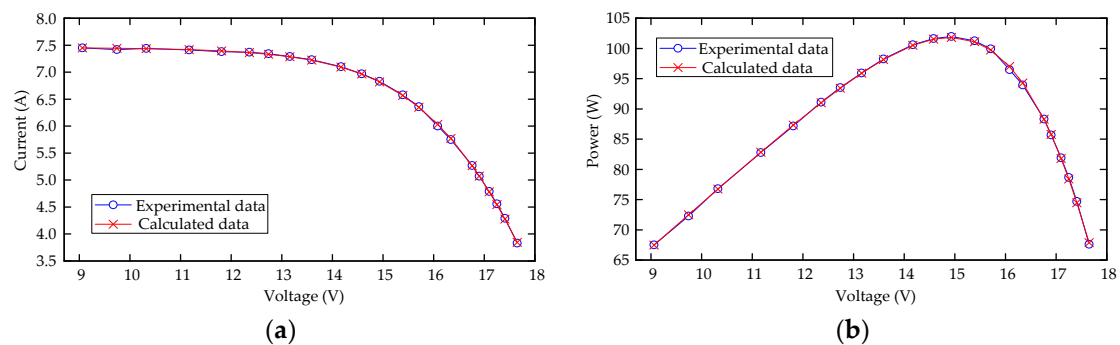
For more evaluation on the quality of the parameters estimated by the proposed ImCSA, the estimated parameters values are put into Equation (10) to reconstruct the calculated current data and calculated power data at experimental voltage point. The experimental data, the calculated data and the IAE are listed in Table 12. It can be found from Table 12 (columns 5 and 7) and the last line of Table 12 that both the IAE and their sum are very small, which provides positive proof that the high accuracy parameter values identified by the ImCSA. Figure 11 plots the I-V and P-V characteristics of the best model parameters estimated by the ImCSA and the experimental data. It is clear from Figure 11 that the calculated data of the PMM of polycrystalline STP6-120/36 panel are highly in coincidence with the experimental data, which further proves the estimated parameters by the ImCSA are very precise.

**Table 11.** Comparison among various parameter estimation algorithms for the PMM of polycrystalline STP6-120/36 panel.

Algorithm	$I_{ph}$ (A)	$I_{sd}$ ( $\mu$ A)	$a$	$R_s$ (m $\Omega$ )	$R_{sh}$ ( $\Omega$ )	OF (RMSE)
ImCSA	7.482778	1.00	1.197729	5.386970	10.00	0.015865799
CSA	7.482777	1.00	1.197733	5.387310	10.00	0.015865806
ABC [11]	7.476291	1.2	1.206992	4.91	9.70	0.019174
CIABC [11]	7.484126	1.29	1.214854	5.1	9.89	0.016286553
Reference [45]	7.4838	1.2	1.2072	4.9	9.745	0.017879

**Table 12.** The calculated results of the proposed ImCSA for the PMM of polycrystalline STP6-120/36 panel.

Item	Experimental Data		Calculated Current Data		Calculated Power Data	
	V (V)	I (A)	$I_{cal}$ (A)	IAE	$P_{cal}$ (W)	IAE
1	17.65	3.83	3.84520015	0.01520015	67.86778268	0.26828268
2	17.41	4.29	4.27711948	0.01288052	74.46465022	0.22424978
3	17.25	4.56	4.54504650	0.01495350	78.40205219	0.25794781
4	17.10	4.79	4.78171108	0.00828892	81.76725939	0.14174061
5	16.90	5.07	5.07559408	0.00559408	85.77753992	0.09453992
6	16.76	5.27	5.26678078	0.00321922	88.27124595	0.05395405
7	16.34	5.75	5.77098920	0.02098920	94.29796346	0.34296346
8	16.08	6.00	6.03372193	0.03372193	97.02224861	0.54224861
9	15.71	6.36	6.34833199	0.01166801	99.73229550	0.18330450
10	15.39	6.58	6.57014416	0.00985584	101.11451856	0.15168144
11	14.93	6.83	6.81958450	0.01041550	101.81639658	0.15550342
12	14.58	6.97	6.96396943	0.00603057	101.53467435	0.08792565
13	14.17	7.10	7.09353516	0.00646484	100.51539327	0.09160673
14	13.59	7.23	7.22168365	0.00831635	98.14268079	0.11301921
15	13.16	7.29	7.28648376	0.00351624	95.89012630	0.04627370
16	12.74	7.34	7.33223712	0.00776288	93.41270088	0.09889912
17	12.36	7.37	7.36266685	0.00733315	91.00256226	0.09063774
18	11.81	7.38	7.39363210	0.01363210	87.31879509	0.16099509
19	11.17	7.41	7.41667187	0.00667187	82.84422481	0.07452481
20	10.32	7.44	7.43458678	0.00541322	76.72493553	0.05586447
21	9.74	7.42	7.44205922	0.02205922	72.48565679	0.21485679
22	9.06	7.45	7.44806806	0.00193194	67.47949662	0.01750338
Sum of IAE				0.23591924		3.46852297

**Figure 11.** Comparisons between the experimental data and calculated data obtained by the proposed ImCSA for the PMM of polycrystalline STP6-120/36 panel: (a) I-V characteristics; (b) P-V characteristics.

### 5.2.2. Case Study 2: PV Module Model with Real Dataset of a Monocrystalline Panel

In this case, to further verify the performance of proposed ImCSA for parameter estimation under a real implementation of monocrystalline panel. The other real dataset is taken into account, where the experimental I–V data from a monocrystalline STM6-40/36 panel at 51 °C [45] contain 18 pairs of voltage and current values. This PV panel is composed of 36 monocrystalline cells in series and dimension of each cell is 38 mm × 128 mm.  $V_{OC} = 21.02$  V,  $I_{SC} = 1.663$  A,  $V_M = 16.98$  V, and  $I_M = 1.50$  A. There are also five unknown parameters needed to be estimated for the PMM of monocrystalline STM6-40/36 panel in this case. The range of each parameter are set as follows:  $I_{ph}$  (A)  $\in [0, 10]$ ,  $I_{sd}$  ( $\mu$ A)  $\in [0, 2]$ ,  $a \in [1, 2]$ ,  $R_s$  (m $\Omega$ )  $\in [0, 10]$ ,  $R_{sh}$  ( $\Omega$ )  $\in [0, 20]$ . The proposed ImCSA is now applied for finding the optimal parameters vector  $\theta$  for the PMM of STM6-40/36 panel based on the experimental I-V data.

The statistics of the OF (RMSE) values for the PMM of the monocrystalline STM6-40/36 panel achieved by the ImCSA and CSA are displayed in Table 13. It is notable that the ImCSA performs better than CSA in terms of all statistical indicators, including the best, mean, median, worst and Std of the OF (RMSE) values in all 30 independent runs. Besides, the ImCSA achieves the best, mean, median, and worst of the OF (RMSE) values as low as  $1.79436329 \times 10^{-3}$  as tabulated in Table 13. Specially, from this table, it can be observed that the ImCSA obtains a Std of  $2.11238634 \times 10^{-14}$ , which is markedly smaller than that calculated by CSA. Then, similarly to previous case, these results prove that the proposed ImCSA is indeed still better than original CSA in terms of accuracy and reliability and improves the performance of CSA. Moreover, the convergence performance for the best run of the proposed ImCSA for parameter estimation of the PMM of monocrystalline STM6-40/36 panel is displayed in Figure 12. Figure 12 shows that the objective value achieved by the ImCSA becomes relatively stable in less than 100 iterations, which is an indication of its fast rate.

Table 14 presents the optimal parameters values and the corresponding objective value of OF (RMSE) for the PMM of monocrystalline STM6-40/36 panel estimated by the ImCSA contrasted with those by CSA and several other parameters estimation methods such as ABC [11], CIABC [11], and Reference [45]. From the OF (RMSE) values in Table 14, it is obvious that the ImCSA achieves the best OF (RMSE) value among these methods, followed by CSA, CIABC, ABC, and Reference [45], which indicates that the proposed ImCSA considerably improves the performance of the original CSA and outperforms all other methods. Consequently, the optimal parameters values determined by the ImCSA are more close to the real ones for the PMM of monocrystalline STM6-40/36 panel, thus the parameters estimated by the proposed ImCSA are accurate.

**Table 13.** Statistics of the OF (RMSE) values for the PMM of monocrystalline STM6-40/36 panel using the proposed ImCSA and CSA.

Algorithm	OF (RMSE)				
	Best	Mean	Median	Worst	Std
ImCSA	$1.79436329 \times 10^{-3}$	$1.79436329 \times 10^{-3}$	$1.79436329 \times 10^{-3}$	$1.79436329 \times 10^{-3}$	$2.11238634 \times 10^{-14}$
CSA	$1.79436368 \times 10^{-3}$	$1.79562418 \times 10^{-3}$	$1.79438763 \times 10^{-3}$	$1.80652265 \times 10^{-3}$	$3.06943955 \times 10^{-6}$

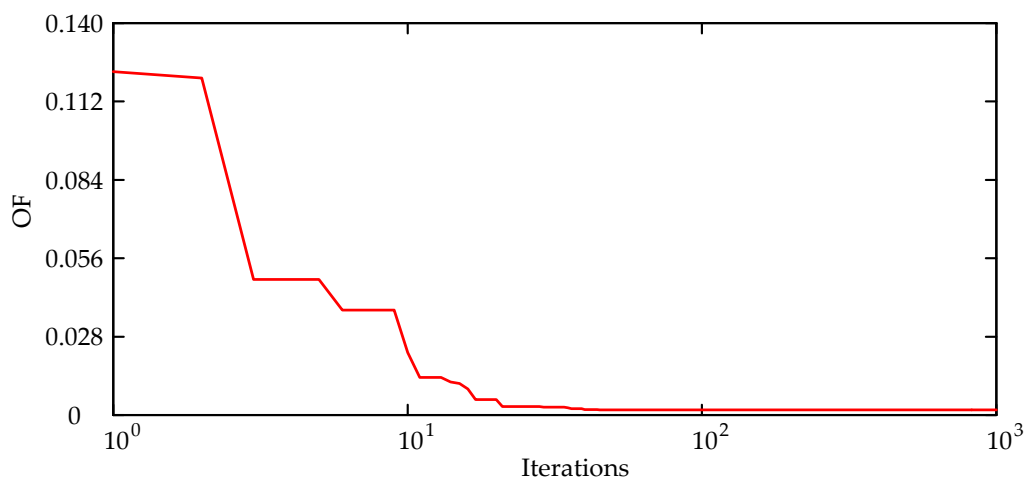


**Figure 12.** Convergence characteristic of the proposed ImCSA for parameter estimation of the PMM of monocrystalline STM6-40/36 panel.

**Table 14.** Comparison among various parameter estimation algorithms for the PMM of monocrystalline STM6-40/36 panel.

Algorithm	$I_{ph}$ (A)	$I_{sd}$ ( $\mu$ A)	$a$	$R_s$ (m $\Omega$ )	$R_{sh}$ ( $\Omega$ )	OF (RMSE)
ImCSA	1.663971	2.0000	1.533499	2.913631	15.840511	0.00179436329
CSA	1.663969	2.0000	1.533497	2.912981	15.840727	0.00179436368
ABC [11]	1.50	1.6644	1.4866	4.99	15.206	0.0018379
CIABC [11]	1.6642	1.6760	1.4976	4.40	15.617	0.001819
Reference [45]	1.6635	1.4142	1.4986	4.879	15.419	0.002181

Similarly, to the previous case, for further establishing the quality of the parameters estimated by the ImCSA, five estimated parameters values are back-substituted into Equation (10) to reconstruct the calculated data of PMM of monocrystalline STM6-40/36 panel. The calculated data and the experimental data are compared in Table 15 for observing the accordance between them and the IAE between experimental and calculated data are also listed in Table 15. It can be observed from Table 15 (columns 5 and 7) and the last line of Table 15 that both the IAE and their sum are very tiny, which gives concrete evidence that the calculated data of PMM of monocrystalline STM6-40/36 panel are in excellent accordance with the experimental data. Additionally, Figure 13 plots the I-V and P-V characteristics of the best model parameters estimated by the proposed ImCSA and the experimental data. This figure clearly portrays that the calculated data are in close agreement with the experimental data, which further demonstrates the high accuracy parameters are achieved again by the proposed ImCSA. Just like the real implementation of polycrystalline panel, the proposed ImCSA is still able to accurately and reliably estimate the parameters of the PMM of monocrystalline panel.

According to the comparison results mentioned above, it demonstrates that ImCSA can obtain similar or better results contrasted with these methods in literature. Thus, it can be used as an accurate and reliable alternative approach for PV models parameter estimation problem.

**Table 15.** The calculated results of the proposed ImCSA for the PMM of monocrystalline STM6-40/36 panel.

Item	Experimental Data		Calculated Current Data		Calculated Power Data	
	V (V)	I (A)	$I_{cal}$ (A)	IAE	$P_{cal}$ (W)	IAE
1	0.118	1.663	1.66345723	0.00045723	0.19628795	0.00005395
2	2.237	1.661	1.65973491	0.00126509	3.71282700	0.00283000
3	5.434	1.653	1.65406328	0.00106328	8.98817985	0.00577785
4	7.260	1.650	1.65068943	0.00068943	11.98400525	0.00500525
5	9.680	1.645	1.64550162	0.00050162	15.92845565	0.00485565
6	11.590	1.640	1.63922838	0.00077162	18.99865687	0.00894313
7	12.600	1.636	1.63364948	0.00235052	20.58398349	0.02961651
8	13.370	1.629	1.62716998	0.00183002	21.75526261	0.02446739
9	14.090	1.619	1.61814834	0.00085166	22.79971010	0.01199990
10	14.880	1.597	1.60286544	0.00586544	23.85063775	0.08727775
11	15.590	1.581	1.58139412	0.00039412	24.65393434	0.00614434
12	16.400	1.542	1.54224568	0.00024568	25.29282922	0.00402922
13	16.710	1.524	1.52122273	0.00277727	25.41963176	0.04640824
14	16.980	1.500	1.49929099	0.00070901	25.45796106	0.01203894
15	17.130	1.485	1.48541163	0.00041163	25.44510128	0.00705128
16	17.320	1.465	1.46585878	0.00085878	25.38867413	0.01487413
17	17.910	1.388	1.38804371	0.00004371	24.85986286	0.00078286
18	19.080	1.118	1.11802403	0.00002403	21.33189856	0.00045856
Sum of IAE				0.02111015		0.27261495

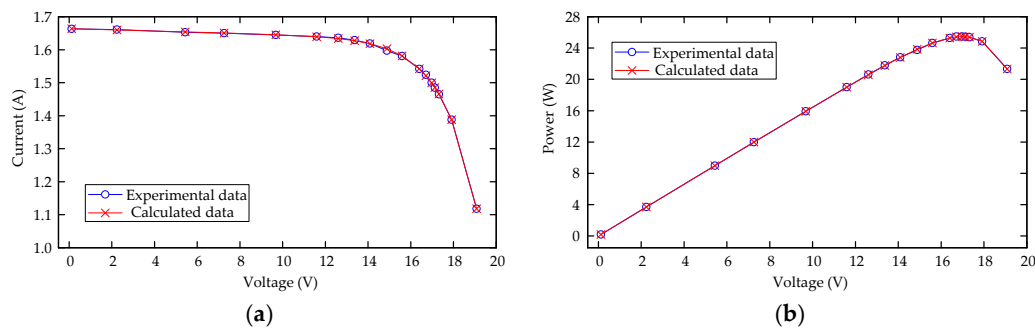


**Figure 13.** Comparisons between the experimental data and calculated data obtained by the proposed ImCSA for the PMM of monocrystalline STM6-40/36 panel: (a) I-V characteristics; (b) P-V characteristics.

Additionally, in order to verify whether the results achieved by the proposed ImCSA are statistically different from the results obtained by original CSA, the two-sample t-test is conducted, and the corresponding *t*-value, *h*, *CI*, and *p*-value are listed in Table 16. A *t*-value being negative means that the results achieved by the ImCSA are comparatively smaller and vice versa. An *h* value of one implies that the performances of the two algorithms are statistically different at the 0.05 significance level, whereas value of zero indicates that the performances are not statistically different. The *CI* is confidence interval. A *p*-value decides the significance level of two algorithms. As can be observed from Table 16, the *t*-values are all negative, the *h* values are all equal to one, all the *CI* values are less than zero and do not contain zero and all the *p*-values are less than 0.05, which indicate that the ImCSA significantly outperforms CSA in all case studies from both groups of experiments. Meanwhile, the Wilcoxon rank-sum test is also performed, and the corresponding *z*-value, *h*, and *p*-value are tabulated in Table 17. From Table 17, we can clearly see that the *z*-values are all negative, the *h* values are all equal to one, and all the *p*-values are extremely less than 0.05, which imply that the ImCSA shows better performance than CSA, in terms of statistical significance. Therefore, the consistent results from both t test and Wilcoxon rank-sum test prove that the proposed ImCSA remarkably enhances the performance of original CSA and is better than CSA and the difference in the results is statistically significant.

**Table 16.** Results of the t test on the data in Tables 1, 4, 7, 10 and 13.

Comparison	Case Study	<i>t</i> -Value	<i>h</i>	<i>CI</i>	<i>p</i> -Value
ImCSA versus CSA	<b>Benchmark Datasets</b>				
	Case Study 1	−2.2130	1	$[-6.5951 \times 10^{-6}, -3.3068 \times 10^{-7}]$	0.03084
	Case Study 2	−4.8129	1	$[-5.2069 \times 10^{-6}, -2.1479 \times 10^{-6}]$	0.000011
	Case Study 3	−2.2325	1	$[-1.0966 \times 10^{-5}, -5.9756 \times 10^{-7}]$	0.02946
	<b>Real Datasets of PV Panels</b>				
	Case Study 1	−3.3177	1	$[-6.0867 \times 10^{-6}, -1.5058 \times 10^{-6}]$	0.00157
Case Study 2	−2.2500	1	$[-2.3827 \times 10^{-6}, -1.3913 \times 10^{-7}]$	0.02826	

**Table 17.** Results of the Wilcoxon rank-sum test on the data in Tables 1, 4, 7, 10 and 13.

Comparison	Case Study	<i>z</i> -Value	<i>h</i>	<i>p</i> -Value
ImCSA versus CSA	<b>Benchmark Datasets</b>			
	Case Study 1	−6.645692	1	$3.017967 \times 10^{-11}$
	Case Study 2	−6.527324	1	$6.695519 \times 10^{-11}$
	Case Study 3	−6.616030	1	$3.689726 \times 10^{-11}$
	<b>Real Datasets of PV Panels</b>			
	Case Study 1	−6.646061	1	$3.010407 \times 10^{-11}$
Case Study 2	−6.645692	1	$3.017967 \times 10^{-11}$	

## 6. Conclusions

This paper proposed a novel improved variant of CSA called ImCSA for solving the PV models parameter estimation problem based on experimental I-V data of real PV cells and modules. As an enhanced version of CSA, the proposed ImCSA combined three strategies with original CSA to improve its performance. First, a strategy named QOBL scheme was employed in the population initialization step of CSA to accelerate its convergence and enhance its solution accuracy. Second, a dynamic adaptation strategy was developed and introduced for the step size without Lévy flight step in original CSA, which makes the step size with zero parameter initialization adaptively change according to the individual nest's fitness value over the course of the iteration and the current iteration number. This strategy is useful for optimization with a faster rate. Third, a dynamic adjustment mechanism for the fraction probability or discovery rate ( $P_a$ ) was proposed to achieve better tradeoff between the exploration and exploitation to increase searching ability. In this paper, the PV models parameter estimation problem was firstly converted into an optimization problem, and an OF was formulated to quantify the overall difference between the simulated and experimental current data. And then, a new improved CSA, named as ImCSA was proposed and applied for solving the problem of estimating the parameters of PV models based on experimental I-V data. Finally, the performance of proposed ImCSA was comprehensively verified on the parameter estimation of different PV models, i.e., SDM, DDM and PMM of various PV cell/modules.

Experimental comparison results from both benchmark datasets and real datasets with CSA and some other parameter estimation methods available literature, such as TLABC, CIABC, MSSO, IJAYA, SATLBO, GOTLBO, EHA-NMS, CARO, IABC, MABC, ABC, BBO-M, MPCOA,  $R_{cr}$ -IJADE, ABSO, HS, SA, PS, CPSO, and GA implied that the proposed ImCSA remarkably enhanced the performance of the original CSA and can obtain similar or better results. And they also showed that our proposed ImCSA was capable of finding the best values of parameters for the PV models in such effective way for giving the best possible approximation to the experimental I-V data of real PV cells and modules. Therefore, the proposed ImCSA can be recommended as a promising option to accurately and reliably estimate PV models parameters.

In future work, we hope the applicability of the proposed ImCSA will be expanded to the FACTS devices allocation problem, power economic dispatch problem and some other real-world optimization problems. Moreover, parameter estimation of PV models under partial shading [46] condition needs to be investigated in further research.

**Author Contributions:** All the authors have contributed in the article. Tong Kang conceived and designed the simulations under the supervision and with the help of Jiangang Yao. Tong Kang performed the experiments, analyzed the data and wrote the paper. Jiangang Yao, Min Jin, Shengjie Yang and ThanhLong Duong reviewed the manuscript and provided some valuable suggestions.

**Acknowledgments:** This work was supported by the National Natural Science Foundation of China (Grant Nos. 51277059, 61374172 and 61773157) and the Outstanding Youth Project of Hunan Provincial Education Department (Grant No. 16B143).

**Conflicts of Interest:** The authors declare no conflict of interest.

## References

1. Askarzadeh, A.; Rezazadeh, A. Parameter identification for solar cell models using harmony search-based algorithms. *Sol. Energy* **2012**, *86*, 3241–3249. [[CrossRef](#)]
2. Oliva, D.; Cuevas, E.; Pajares, G. Parameter identification of solar cells using artificial bee colony optimization. *Energy* **2014**, *72*, 93–102. [[CrossRef](#)]
3. Askarzadeh, A.; Rezazadeh, A. Extraction of maximum power point in solar cells using bird mating optimizer-based parameters identification approach. *Sol. Energy* **2013**, *90*, 123–133. [[CrossRef](#)]
4. Yuan, X.; He, Y.; Liu, L. Parameter extraction of solar cell models using chaotic asexual reproduction optimization. *Neural Comput. Appl.* **2015**, *26*, 1227–1239. [[CrossRef](#)]

5. Jordehi, A.R. Parameter estimation of solar photovoltaic (PV) cells: A review. *Renew. Sustain. Energy Rev.* **2016**, *61*, 354–371. [CrossRef]
6. *Snapshot of Global Photovoltaic Markets*, 5th ed. IEA-PVPS T1-31. 2017. Available online: [http://www.iaa-pvps.org/fileadmin/dam/public/report/statistics/IEA-PVPS\\_-\\_A\\_Snapshot\\_of\\_Global\\_PV\\_-\\_1992-2016\\_\\_1\\_.pdf](http://www.iaa-pvps.org/fileadmin/dam/public/report/statistics/IEA-PVPS_-_A_Snapshot_of_Global_PV_-_1992-2016__1_.pdf) (accessed on 6 March 2018).
7. Reinders, A.; van Sark, W.; Verlinden, P. Introduction. In *Photovoltaic Solar Energy: From Fundamentals to Applications*; Reinders, A., Verlinden, P., van Sark, W., Freundlich, A., Eds.; John Wiley & Sons, Ltd.: Chichester, UK, 2017; pp. 1–12.
8. Jordehi, A.R. Time varying acceleration coefficients particle swarm optimisation (TVACPSO): A new optimisation algorithm for estimating parameters of PV cells and modules. *Energy Convers. Manag.* **2016**, *129*, 262–274. [CrossRef]
9. Humada, A.M.; Hojabri, M.; Mekhilef, S.; Hamada, H.M. Solar cell parameters extraction based on single and double-diode models: A review. *Renew. Sustain. Energy Rev.* **2016**, *56*, 494–509. [CrossRef]
10. Chen, X.; Yu, K.; Du, W.; Zhao, W.; Liu, G. Parameters identification of solar cell models using generalized oppositional teaching learning based optimization. *Energy* **2016**, *99*, 170–180. [CrossRef]
11. Oliva, D.; Ewees, A.A.; Aziz, M.A.E.; Hassanien, A.E.; Cisneros, M.P. A chaotic improved artificial bee colony for parameter estimation of photovoltaic cells. *Energies* **2017**, *10*, 865. [CrossRef]
12. Jain, A.; Kapoor, A. Exact analytical solutions of the parameters of real solar cells using Lambert W-function. *Sol. Energy Mater. Sol. Cells* **2004**, *81*, 269–277. [CrossRef]
13. Lun, S.X.; Du, C.J.; Guo, T.T.; Wang, S.; Sang, J.S.; Li, J.P. A new explicit I-V model of a solar cell based on Taylor's series expansion. *Sol. Energy* **2013**, *94*, 221–232. [CrossRef]
14. Easwarakhanthan, T.; Bottin, J.; Bouhouch, I.; Boutrit, C. Nonlinear minimization algorithm for determining the solar cell parameters with microcomputers. *Int. J. Sol. Energy* **1986**, *4*, 1–12. [CrossRef]
15. Chatterjee, A.; Keyhani, A.; Kapoor, D. Identification of photovoltaic source models. *IEEE Trans. Energy Convers.* **2011**, *26*, 883–889. [CrossRef]
16. Shongwe, S.; Hanif, M. Gauss-Seidel iteration based parameter estimation for a single diode model of a PV module. In Proceedings of the 2015 IEEE Electrical Power and Energy Conference (EPEC), London, ON, Canada, 26–28 October 2015; pp. 278–284.
17. Tossa, A.K.; Soro, Y.M.; Azoumah, Y.; Yamegueu, D. A new approach to estimate the performance and energy productivity of photovoltaic modules in real operating conditions. *Sol. Energy* **2014**, *110*, 543–560. [CrossRef]
18. Laudani, A.; Riganti Fulginei, F.; Salvini, A. High performing extraction procedure for the one-diode model of a photovoltaic panel from experimental I-V curves by using reduced forms. *Sol. Energy* **2014**, *103*, 316–326. [CrossRef]
19. Jervase, J.A.; Bourdoucen, H.; Al-Lawati, A. Solar cell parameter extraction using genetic algorithms. *Meas. Sci. Technol.* **2001**, *12*, 1922–1925. [CrossRef]
20. Wei, H.; Cong, J.; Lingyun, X.; Deyun, S. Extracting solar cell model parameters based on chaos particle swarm algorithm. In Proceedings of the 2011 International Conference on Electric Information and Control Engineering (ICEICE), Wuhan, China, 15–17 April 2011; pp. 398–402.
21. Alhajri, M.F.; El-Naggar, K.M.; Alrashidi, M.R.; Al-Othman, A.K. Optimal extraction of solar cell parameters using pattern search. *Renew. Energy* **2012**, *44*, 238–245. [CrossRef]
22. AlRashidi, M.R.; AlHajri, M.F.; El-Naggar, K.M.; Al-Othman, A.K. A new estimation approach for determining the I-V characteristics of solar cells. *Sol. Energy* **2011**, *85*, 1543–1550. [CrossRef]
23. El-Naggar, K.M.; AlRashidi, M.R.; AlHajri, M.F.; Al-Othman, A.K. Simulated Annealing algorithm for photovoltaic parameters identification. *Sol. Energy* **2012**, *86*, 266–274. [CrossRef]
24. Askarzadeh, A.; Rezaazadeh, A. Artificial bee swarm optimization algorithm for parameters identification of solar cell models. *Appl. Energy* **2013**, *102*, 943–949. [CrossRef]
25. Gong, W.; Cai, Z. Parameter extraction of solar cell models using repaired adaptive differential evolution. *Sol. Energy* **2013**, *94*, 209–220. [CrossRef]
26. Yuan, X.; Xiang, Y.; He, Y. Parameter extraction of solar cell models using mutative-scale parallel chaos optimization algorithm. *Sol. Energy* **2014**, *108*, 238–251. [CrossRef]
27. Niu, Q.; Zhang, L.; Li, K. A biogeography-based optimization algorithm with mutation strategies for model parameter estimation of solar and fuel cells. *Energy Convers. Manag.* **2014**, *86*, 1173–1185. [CrossRef]

28. Jamadi, M.; Mehdi, F.M. Very accurate parameter estimation of single- and double-diode solar cell models using a modified artificial bee colony algorithm. *Int. J. Energy Environ. Eng.* **2015**, *7*, 13–25. [[CrossRef](#)]
29. Wang, R.; Zhan, Y.; Zhou, H. Application of artificial bee colony in model parameter identification of solar cells. *Energies* **2015**, *8*, 7563–7581. [[CrossRef](#)]
30. Chen, Z.; Wu, L.; Lin, P.; Wu, Y.; Cheng, S. Parameters identification of photovoltaic models using hybrid adaptive Nelder-Mead simplex algorithm based on eagle strategy. *Appl. Energy* **2016**, *182*, 47–57. [[CrossRef](#)]
31. Yu, K.; Chen, X.; Wang, X.; Wang, Z. Parameters identification of photovoltaic models using self-adaptive teaching-learning-based optimization. *Energy Convers. Manag.* **2017**, *145*, 233–246. [[CrossRef](#)]
32. Yu, K.; Liang, J.J.; Qu, B.Y.; Chen, X.; Wang, H. Parameters identification of photovoltaic models using an improved JAYA optimization algorithm. *Energy Convers. Manag.* **2017**, *150*, 742–753. [[CrossRef](#)]
33. Lin, P.; Cheng, S.; Yeh, W.; Chen, Z.; Wu, L. Parameters extraction of solar cell models using a modified simplified swarm optimization algorithm. *Sol. Energy* **2017**, *144*, 594–603. [[CrossRef](#)]
34. Chen, X.; Xu, B.; Mei, C.; Ding, Y.; Li, K. Teaching-learning-based artificial bee colony for solar photovoltaic parameter estimation. *Appl. Energy* **2018**, *212*, 1578–1588. [[CrossRef](#)]
35. Wolpert, D.H.; Macready, W.G. No free lunch theorems for optimization. *IEEE Trans. Evol. Comput.* **1997**, *1*, 67–82. [[CrossRef](#)]
36. Yang, X.S.; Deb, S. Cuckoo search via Lévy flights. In Proceedings of the 2009 World Congress on Nature & Biologically Inspired Computing, 2009 (NaBIC 2009), Coimbatore, India, 9–11 December 2009; pp. 210–214.
37. Ljouad, T.; Amine, A.; Rziza, M. A hybrid mobile object tracker based on the modified cuckoo search algorithm and the kalman filter. *Pattern Recogn.* **2014**, *47*, 3597–3613. [[CrossRef](#)]
38. Fister, I., Jr.; Fister, D.; Fister, I. A comprehensive review of cuckoo search: Variants and hybrids. *Int. J. Math. Model. Numer. Optim.* **2013**, *4*, 387–409.
39. Kang, T.; Yao, J.; Duong, T.L.; Yang, S.; Zhu, X. A hybrid approach for power system security enhancement via optimal installation of flexible AC transmission system (FACTS) devices. *Energies* **2017**, *10*, 1305. [[CrossRef](#)]
40. Tizhoosh, H.R. Opposition-based learning: A new scheme for machine intelligence. In Proceedings of the 2005 International Conference on Computational Intelligence for Modelling, Control and Automation, and International Conference on Intelligent Agents, Web Technologies and Internet Commerce (CIMCA-IAWTIC'05), Vienna, Austria, 28–30 November 2005; pp. 695–701.
41. Rahnamayan, S.; Tizhoosh, H.R.; Salama, M.M.A. Opposition-based differential evolution. *IEEE Trans. Evol. Comput.* **2008**, *12*, 64–79. [[CrossRef](#)]
42. Xu, Q.; Wang, L.; Wang, N.; Hei, X.; Zhao, L. A review of opposition-based learning from 2005 to 2012. *Eng. Appl. Artif. Intell.* **2014**, *29*, 1–12. [[CrossRef](#)]
43. Rahnamayan, S.; Tizhoosh, H.R.; Salama, M.M.A. Quasi-oppositional differential evolution. In Proceedings of the 2007 IEEE Congress on Evolutionary Computation (CEC 2007), Singapore, 25–28 September 2007; pp. 2229–2236.
44. Ergezer, M.; Simon, D. Mathematical and experimental analyses of oppositional algorithms. *IEEE Trans. Cybern.* **2014**, *44*, 2178–2189. [[CrossRef](#)] [[PubMed](#)]
45. Tong, N.T.; Pora, W. A parameter extraction technique exploiting intrinsic properties of solar cells. *Appl. Energy* **2016**, *176*, 104–115. [[CrossRef](#)]
46. Pannebakker, B.B.; de Waal, A.C.; van Sark, W.G.J.H.M. Photovoltaics in the shade: One bypass diode per solar cell revisited. *Prog. Photovolt. Res. Appl.* **2017**, *25*, 836–849. [[CrossRef](#)]

